Adaptive steering wheel stiffness in driving with Haptic Shared Control

MSc. Thesis H.M. Zwaan

Adaptive steering wheel stiffness in driving with Haptic Shared Control

by

H.M. Zwaan

to obtain the degree of Master of Science
at the Delft University of Technology,
to be defended publicly on Friday August 3, 2018 at 13:30.

Student number:	4023102	
Project duration:	June, 2017 – July, 2018	
Thesis committee:	Prof. dr. ir. D. A. Abbink,	TU Delft, supervisor
	Dr. ir. S. M. Petermeijer,	TU Delft, supervisor
	Dr. ir. J. C. F. de Winter,	TU Delft, external member

An electronic version of this thesis is available at `http://repository.tudelft.nl/`.

TU Delft

Preface

This thesis is, in its core, investigating a fundamental part of technology. It not only investigates how technology can be designed such that it benefits us but also how it can interact with us in a way that we like. Developing good technology in itself does not result in good products, people have to love using a technology to make it a lasting success. That, in my view, is what makes Haptic Shared Control better than traded control in automated vehicles: it has the superior driver interaction.

I want to express my appreciation for my daily supervisors David Abbink and Bastiaan Petermeijer, who not only proved me with support and feedback throughout the project, but also provided desks in their offices for graduate students to work in close collaboration with themselves, PhD candidates and other graduate students. I believe this environment promotes healthy discussion, provides inspiration and effective communication. I want to thank all the members of the TUDelft Haptic's Lab with a special mention to Timo Melman for his insights and feedback throughout the project, and above all to Sarvesh Kolekar who went above and beyond what was expected to help me perform the experiments for this thesis.

Thanks to all the master students in the lab and the great small social community we have shared together, special thanks to Fokke Zwaan and Bram van Os for proof-reading my work and providing sharp feedback. And thanks to both my parents for letting me choose my preferred field of study, twice over, and supporting me throughout.

H.M. Zwaan
Delft, July 2018

Contents

1

Research Paper

Adaptive steering wheel stiffness in driving with Haptic Shared Control

Hugo M. Zwaan, Sebastianus M. Petermeijer, Sarvesh B. Kolekar and David A. Abbink

***Abstract*—Driving with Haptic Shared Control (HSC) provides an alternative for traditional traded control in human-controller interaction. Whilst driving, control is shared between the driver and the controller by translating the controller's desired steering input to additional torques on the steering wheel. Literature provides several guidelines for the tuning of these torques but not for the tuning of the interaction stiffness around the controller's desired steering input: the Level of Haptic Authority (LoHA), this is usually kept constant. High LoHA tunings have beneficial effects on the driver performance but result in high conflict torques and negatively impact the driver acceptance. In this study two adaptive LoHA algorithms are proposed based on Time to Lane Crossing (TLC). By increasing the LoHA in critical, low-TLC, scenarios these should improve performance while also allowing for a larger steering freedom and low conflicts in safe scenarios. The adaptive LoHA is applied symmetrically (bi-directional) and asymmetrically (only in the direction of the low TLC). The adaptive algorithms are compared to manual driving, a low and a high static LoHA tuning in a within-subject driving simulator study. Fourteen participants performed a lane keeping task in which lane width varied to influence the safety margins and TLC. While driving with adaptive LoHA, the mean conflict torque was significantly lower for the adaptive algorithms than for the high stiffness controller and participants experienced lower workloads. However, no difference was found between the symmetric and asymmetric LoHA controller. These results show that adaptive LoHA based on TLC is an effective way to achieve a similar performance as with static LoHA but with lower conflicts and a lower workload.**

***Index Terms*—Haptic Shared Control, Adaptive, Level of Haptic Authority, Human-Machine interaction, driving simulator.**

I. Introduction

Haptic Shared Control (*HSC*) implements the control action of an autonomous driving system through the steering wheel, allowing for a continuous interaction between the driver and the vehicle in which decision making and intent are translated into added torques on the steering wheel [1]. By keeping the driver actively engaged in the control loop, the interactions mitigates the "pitfalls of automation" related to supervised autonomous driving [2, 3] while benefiting from an increased driving performance [4, 5, 6, 7] and reduced workload [5, 6, 3]. By using a haptic steering wheel rather than trading control [8] or mixing the inputs at the wheels [9] the driver is also more aware of the controller actions and intent [1, 5, 10].

In its simplest form, HSC is achieved by pure force feedback: a torque that turns the steering wheel towards the desired steering wheel angle [7, 11]. An alternative approach is adding stiffness feedback through a virtual spring around the controller's desired steering wheel angle. This creates torques in response to deviations from this angle. This is analogous to a human rotating the steering wheel. Who can perform the same steering trajectory with a low co-contraction (low stiffness) or with high co-contraction (high stiffness). The two are combined in force-stiffness feedback [12, 13] that both actively steers the wheel, shifts the neutral angle and changes the stiffness.

This artificial stiffness around the controller's desired steering angle and is called the Level of Haptic Authority (LoHA). The stiffer the LoHA is, the harder it becomes to deviate from the controller's actions and vice versa. By adjusting the LoHA, the authority can be shifted between the driver and the controller [1]. As the stiffness approaches infinity it becomes impossible to overrule the system, effectively turning the shared controller into a fully autonomous controller.

In literature there are some guidelines of how to tune the LoHA, such as to the neuromuscular admittance [14, 15] or personal trajectory [16], but most tunings are made heuristically [3, 17, 18]. High LoHA controllers yield the biggest performance improvements in terms of lateral position, safety margins and variability [2][17][3] but result in forceful corrections. Drivers can get annoyed by these kind of corrections because they do not always perceive anything wrong with their performance [19]. As drivers 'fight' the system with increasing torques, this results in lower user acceptance [10][15][3], heightening the chance of these systems being disused [20]. It is for this reason that low LoHA controllers are preferred by drivers [16].

It has been suggested that a single LoHA value might not suffice [21][1] and that an adaptive LoHA might be a better solution. Adaptive LoHA based on lateral error, with respect to the reference, has even been implemented by Abbink and Mulder (2009) [13], but they found a negative effect on performance because the controller enlarged conflicts between the driver and the reference. Because human behaviour is described as satisficing rather than optimising [22][23] it is hypothesised that a haptic shared controller should allow for this behaviour: the controller should be compliant when driver performance is satisfactory, reducing the size of trivial conflicts and improving acceptance, whilst having the performance benefits of a high stiffness controller in critical situations.

In unaided driving, task-dependent steering wheel stiffness has been investigated by Mulder et al. [24] who showed that driving on different road conditions benefits from different steering wheel stiffnesses. In HSC, force feedback, not LoHA, has been made adaptable [11] by grip strength or adaptive to lane position [6]. In a similar manner LoHA can be made dependent on a criticality function [1] [12] or performance [25]. These studies show that adaptive support outperforms static tunings of values.

Petermeijer [3] implemented a discrete adaptive controller in the form of a bandwidth controller based on lateral road position with had a deadband in the middle of the road. He found that drivers disliked the discrete nature of the controller because it was difficult to predict the controller actions and also resulted in oscillatory behaviour around the switching threshold. A similar resentment to discrete feedback was found in a study by Suzuki [26]. In the light of these results this study will explore a smooth, continuous function to describe the LoHA.

At the basis of satisficing driving lie safety margins and the perception of risk [27][28]; an intuitive way to interpret safety margins is through the Time to Lane Crossing (*TLC*) [29], which captures a combination of risk related factors in a single value, namely: Velocity, Road Width, Curvature, Lateral Position, and Heading. It has furthermore been shown that the adaptation of driver arm-admittance, the human counterpart of LoHA, correlates to TLC [30], meaning a TLC based LoHA mimics human behaviour. Therefore adaptive LoHA will be defined as a function of the TLC.

The goal of this research is to investigate if adaptive LoHA can yield the performance benefits of high LoHA controllers while reaching the user acceptance ratings of low LoHA controllers. This paper first discusses the mathematical implementation of LoHA in a Haptic Shared Controller and then lays out the design of algorithms that adapt the LoHA based on TLC. It continues to report the findings in a simulator study with these two algorithms.

II. Controller Design

There are several controller architectures that have implemented LoHA, such as a compensatory controller lookahead controller [6] or a two-point controller [16]. Defining for these controllers is their corrective behaviour, they apply torques proportional to an error between the desired and actual trajectories; this means they do not provide any support when the error is zero. The Four Design Choice Architecture (*FDCA*) addresses this point by providing support through a separate feedforward loop, even when there is no offset from the reference [31].

A. Four Design Choice Architecture

The FDCA is a controller architecture that revolves around four design parameters than determine the controller behaviour, see Figure 1:

- Human Compatible Reference (*HCR*), a predetermined reference trajectory for the road.
- Level of Haptic Support *(LoHS*), a feedforward percentage of torques required to follow the HCR.
- Strength of Haptic Feedback (*SoHF*), the feedback gains that correct deviations from the HCR.
- Level of Haptic Authority (*LoHA*), a virtual spring around the controller's desired steering wheel angle.

Previous work by Wyzen [32] simulated the FDCA feedforward and feedback channels, Scholtens [33] details the generation and individualisation of the HCR. Their work lies at the basis of the mathematical models used in this study. This study will detail the previously unexplored implementation of the LoHA in the FDCA architecture and will also touch upon the design of, and interaction with, the LoHS and SoHF.

1) Human Compatible Reference: The Human Compatible Reference is the actual trajectory that the controller tries to follow. For this research the HCR is not investigated, rather the implementation of Scholtens [33] is used. She generated the HCR a priori with a simulated car, controlled by a lookahead controller based on Saleh [34] and a tangent point as determined by Boer [35]. The HCR contains a record of all of the feedforward commands along the road and its trajectory is the reference for the feedback controller. Scholtens' lookahead controller's individualised behaviour is determined by five parameters, the remaining parameters are taken from Saleh. These parameters are listed in Table I at the end of this section. The parameters used in this study were the same as the One-Size-Fits-All (OSFA) controller for right turns as used by Scholtens. These parameters result in an HCR that is closest to the average trajectory of all participants in her experiment. Instead of recording the controller torques, this study will record the desired steering wheel angle from Saleh's controller in order to be able to apply LoHA around this angle, the feedforward controller converts these angles to torques using an inverse model of the steering wheel dynamics.

2) Steering Wheel Dynamics: The steering wheel is modelled as a simple mass-spring damper system

$$\ddot{\theta} = \frac{1}{I_{sw}} \left(\tau - B_{sw}\dot{\theta} - K_{sw}\theta \right) \tag{1}$$

A Laplace transformation (2) is applied to obtain the transfer function (4) of the steering wheel dynamics.

$$F(s) = \int_0^\infty f(t)e^{-st}dt \tag{2}$$

$$H(s) = \frac{Y(s)}{X(s)} \tag{3}$$

$$H_{sw}(s) = \frac{1}{I_{sw} \cdot s^2 + B_{sw} \cdot s + K_{sw}} \tag{4}$$

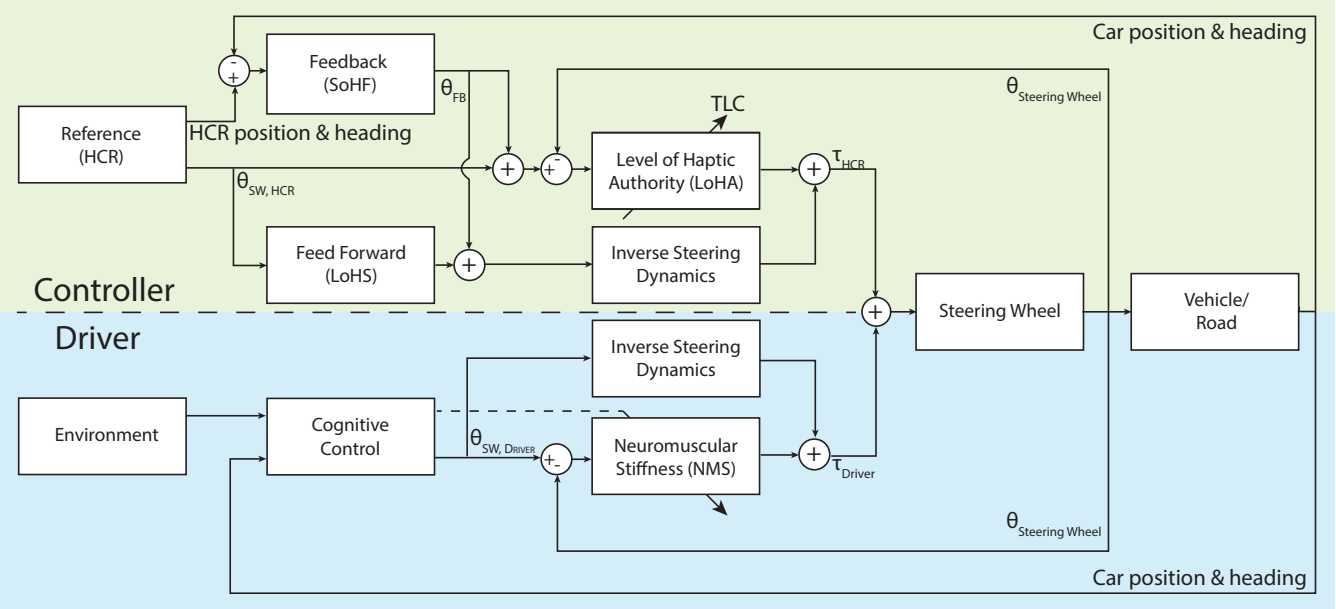

Fig. 1. FDCA architecture, the Level of Haptic Authority (LoHA) is a TLC dependent stiffness around the steering wheel angle of the feedforward and feedback controller. The driver can in turn adapt his own neuromuscular stiffness to reject the controller action.

Through inversion a transfer function of the inverse steering wheel dynamics is obtained. This transfer function however, is improper: the order of the numerator exceeds the order of the denominator, and thus this system is non-causal. To mend this a second order Butterworth filter [36] is added (5). The filter's cut-off frequency (ω_c) is set at 3 Hz, the natural cut-off frequency of the human response [37].

$$H_{butw}(s) = \frac{1}{(\frac{s}{\omega_c})^2 - (\lambda_1 + \lambda_2)\frac{s}{\omega_c} + \lambda_1\lambda_2} \tag{5}$$

$$H_{SW}^{-1}(s) = \frac{I_{sw} \cdot s^2 + B_{sw} \cdot s + K_{sw}}{(\frac{s}{\omega_c})^2 - (\lambda_1 + \lambda_2)\frac{s}{\omega_c} + \lambda_1\lambda_2} \tag{6}$$

$$\lambda_{k(1,2)} = e^{\frac{i\pi}{2n}(2k-1+n)} \tag{7}$$

3) Level of Haptic Support: The Level of Haptic Support (LoHS) was originally defined by Van Paassen [31] as the percentage of the feedforward steering action that is being performed by the controller. At 0% the controller has no feedforward component and acts only on the feedback controller, at 100% the controller performs all feedforward actions which means that without disturbance it will perfectly follow the HCR and basically act like a fully autonomous car. While originally implemented by Wyzen and Scholtens with a torque recording as in (8). The adjusted (9) is used, based on the recorded steering wheel angle θ_{HCR}.

$$\tau_{FF} = \lambda_{LoHS} \cdot \tau_{hcr} \tag{8}$$

$$= \lambda_{LoHS} \cdot H_{sw}^{-1} \cdot \theta_{HCR} \tag{9}$$

The LoHS should be an intermediate value between 0 and 100% as to actively engage the driver in the steering activity and prevent human factors issues, It was heuristically tuned to 80% for this study.

4) Strength of Haptic Feedback: The Strength of Haptic Feedback (SoHF) aims to correct deviations from the HCR. Wyzen used a proportional feedback controller on the current lateral error Δ_s and current heading error Δ_ψ between the car and the HCR [32]. This controller consists of two feedback gains for the lateral and heading error notated as: K_s and K_ψ. In order to obtain the resulting steady-state steering wheel angle, this torque is multiplied by the inverse steering wheel stiffness as in Equation (10).

$$\theta_{FB} = \frac{K_y \cdot \Delta_y + K_\psi \cdot \Delta_\psi}{K_{sw}} \tag{10}$$

$$\tau_{FB} = H_{sw}^{-1} \cdot \theta_{FB} \tag{11}$$

The feedback gains were heuristically tuned to effectively steer the vehicle back to the reference trajectory in a stable manner whilst providing comfortable levels of feedback torque allowing for human deviation from the HCR.

5) Level of Haptic Authority: In this study the *Level of Haptic Authority* (LoHA) will be introduced to the FDCA architecture; a virtual spring that acts on the steering wheel around the desired steering wheel angle of the FDCA controller [1]. In the following analysis the LoHA will be decomposed into a base steering wheel stiffness K_{sw}, or minimum LoHA value, and a stiffness that can be artificially added on top, K_{added}. This means that with equal damping and inertia the torque as a result of the LoHA is described by Equation (13).

Coupling the LoHA with the equations for feedforward (9) and the feedback (11) torques results in the following mathematical description.

$$K_{LoHA} = K_{sw} + K_{added} \tag{12}$$

$$\tau_{LoHA} = (\theta_{co} - \theta_{sw}) \cdot \left(H_{sw}^{-1} + \frac{K_{added}}{H_{filt}} \right) \tag{13}$$

$$\tau_{total} = \tau_{FF} + \tau_{FB} + \tau_{LoHA} \tag{14}$$

$$\tau_{total} = \lambda_{LoHS} \cdot H_{sw}^{-1} \cdot \theta_{HCR} + H_{sw}^{-1} \cdot \theta_{FB} ... \\ ... + (\theta_{FF} + \theta_{FB} - \theta_{sw}) \cdot \left(H_{sw}^{-1} + \frac{K_{added}}{H_{filt}} \right) \tag{15}$$

B. Simulation of LoHA controller

To evaluate the response of the steering wheel angle, controller, and driver torques to different values of the LoHA and LoHS and different controller and driver signals, the steering wheel model was simulated with a virtual driver. The driver's dynamics are simulated by a separate mass-spring-damper system, for simplicity reasons the human inertia and dampening are the same as those of the steering wheel. The controller has no estimates of the human inertia, dampening or stiffness while the human model does anticipate the steering wheel's inertia and dampening because of system identification naturally performed by humans [38]. In the simulation both the controller and driver make the exact same steering movement but the human command is delayed by five seconds, this results in consecutive sections of disagreement and agreement between the controller and the driver. In Figures 2 and 3 the resulting steering wheel angle and torque responses can be observed.

The following observations are made during disagreeing steering angles: LoHA is an effective way to shift the resulting steering wheel angle towards the controller's desired angle. However, if the driver compensates his own admittance this effect on the trajectory is neutralised while the conflicting torques increase. The LoHS also shifts the followed trajectory between controller and driver but this effect diminishes as LoHA increases with respect to the base steering wheel stiffness. During agreement of the steering angles the LoHA has no effect on either the steering angle or the torques; in this case the LoHS fully determines how the torques are divided between the controller and driver. This confirms the LoHA can be used to shift the steering wheel response between controller and driver during conflicts without affecting torques in agreement, while still allowing for the driver to overrule the controller by adapting their own admittance.

Time to Lane Crossing: Three methods of determining the TLC are found in literature. The simplest method extrapolates the current vehicle heading, the most commonly used method of Godthelp [39] takes into account the current yaw rate in the extrapolation and a novel method of Boer[23] that takes into account an uncertainty range of yaw rates and calculates a cone-like swath rather than a single value.

The calculation methods of Boer[23] were used in this research because the TLC swath gives more information about the margins around the current trajectory, the TLC swath can be seen as a crude interpretation of a Safe Field of Travel as described by [27][28]. This extra information opens up the possibility of using directional stiffness feedback, a concept that will be elaborated on in section II-C.

C. Adaptive Stiffness

Adaptive stiffness had been proposed in the past [1][19], adaptive stiffness meaning that the K_{LoHA} is defined as a function of some (set of) variable(s) $K_{LoHA}(x)$. The extreme values of the function are determined first:

The lower LoHA limit is chosen to be the standard steering wheel stiffness of the simulator's vehicle model (0.0085 [Nm/deg]), in this situation the haptic controller only shifts the neutral point compared to manual driving. The upper limit was set at (0.0255 [Nm/deg]), three times the base stiffness, this value was heuristically determined during the pilot study as the highest multiple of the base stiffness before participants would subjectively report dissatisfaction.

A two second threshold for the adaptive algorithm was based on research by Godthelp [29] who reports that drivers

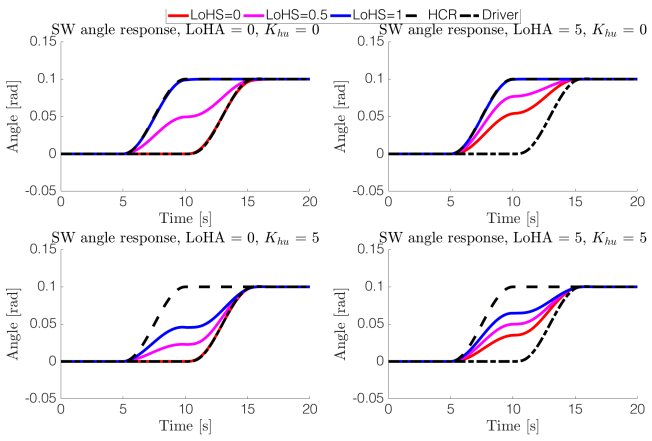

Fig. 2. Steering angle response for different ratios of LoHS, LoHA and driver stiffness

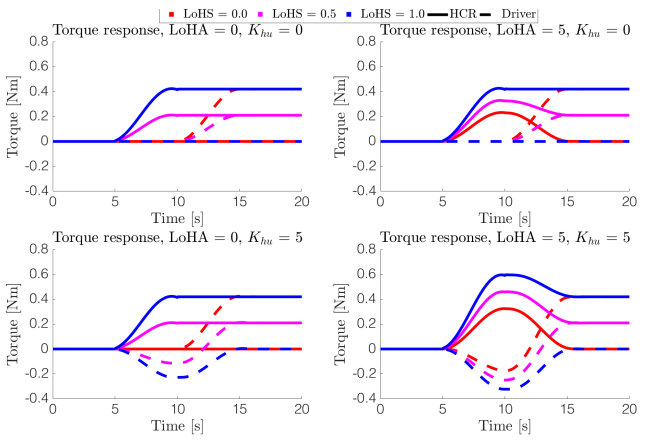

Fig. 3. Driver and controller torque responses for different ratios of LoHS, LoHA and driver stiffness

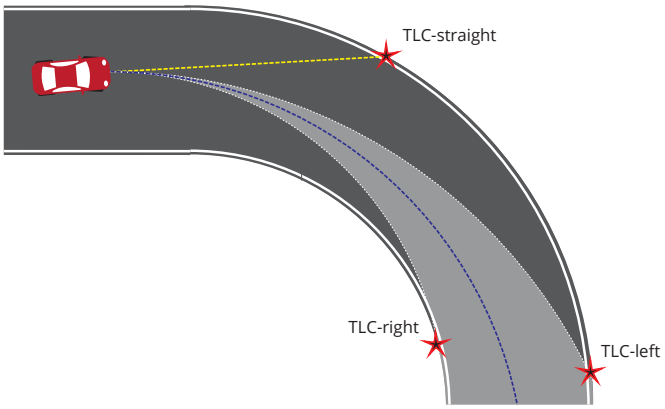

Fig. 4. Illustration of three different TLC calculations: Yellow - extrapolation of vehicle heading ; Blue - extrapolation of yaw rate ; White - yaw uncertainty swath. The latter is used in this research.

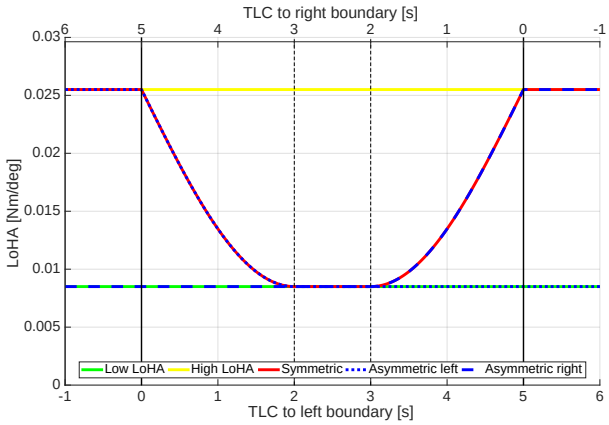

Fig. 5. LoHA profile as a function of the TLC. Note the difference between the asymmetric controller steering left or right.

on average take corrective measures at a TLC of about 1.3 seconds (SD = 0.43 [s]) while driving on a straight road. This means that a two second TLC is a satisfactory performance for about 95% of people. A two second threshold was also found as the time by which $> 95\%$ of drivers have responded to static roadside stimuli [40], furthermore a safety margin of two seconds is advised by Dutch road authorities.

Because Petermeijer [3] showed that drivers dislike sudden transitions in LoHA, the adaptive LoHA is modelled with a partial cosine to give a smooth transition over the full range of positive TLC's. At the point of lane departure ($t_{TLC} \leq 0$), the stiffness reaches its maximum value and does not increase further. This design choice is motivated by maintaining ultimate authority for the driver, in real driving the driver should always be capable of overruling the system and may have ulterior motives to leave the lane the system does not comprehend [41].

$$K_{LoHA} = \ldots$$
$$\begin{cases} K_{min} + K_{add} & , \quad t_{TLC} \leq 0 \\ K_{min} + K_{add}\left(1 + \cos(t_{TLC} + 2)\frac{\pi}{4}\right) & , \quad 2 \geq t_{TLC} > 0 \\ K_{min} & , \quad t_{TLC} > 2 \end{cases} \tag{16}$$

Two adaptive controllers: A symmetric adaptive stiffness is the straightforward implementation of adaptive stiffness as proposed by [21][1] and shifts authority towards the controller regardless of driver intent. However, it is hypothesised that drivers might dislike a symmetric system exactly because it limits their steering actions in all directions; when the criticality is high on only one side of the vehicle it can be desirable to implement an asymmetric stiffness algorithm. Such an algorithm has a high stiffness towards low TLC areas but allows for unhindered steering actions towards low TLC and safety. The TLC swath of Boer[23] makes it possible to separately evaluate the TLC and criticality in either direction of the car.
The same adaptive stiffness profile is used as with adaptive symmetric LoHA but rather than being based on the lowest TLC, the independent value is based on the lowest TLC in the direction of the human torque. The algorithm ran at 100 Hz to ensure participants, who have a just noticeable difference for physical signals of only 10 Hz [42], would not experience any delay in the controller.

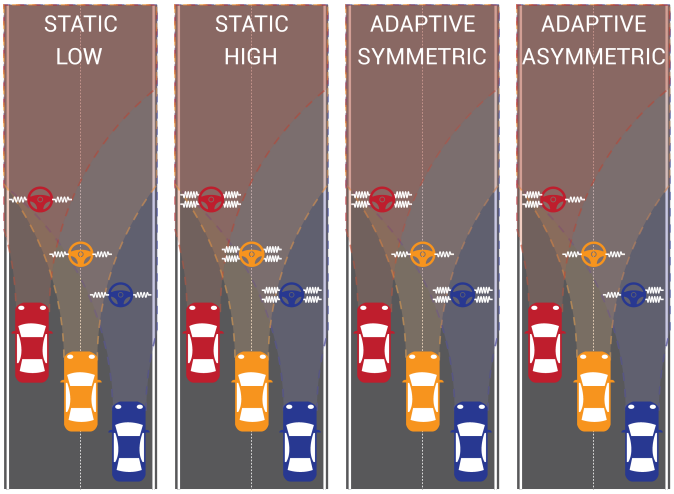

Fig. 6. Visualisation of the steering wheel stiffness of the different LoHA regimes in different road positions. The springs indicate a high or low stiffness for each algorithm in that steering direction, the coloured cones indicate the corresponding TLC swaths.

TABLE I
PARAMETER VALUES USED FOR GENERATION OF THE HUMAN COMPATIBLE REFERENCES (HCR).

Far Gain (K_p)	2.5 [Nm/m]
Near Gain (K_c)	4.0 [Nm/m]
Begin Steering Distance (BSD)	12.5 [m]
End Steering Distance (ESD)	55 [m]
t_{far}	3.5 [s]
T_I	1 [-]
T_L	3 [-]
τ_p	0.03 [s]
K_r	0.3 [-]
K_t	0.5 [-]
T_N	0.1 [-]

D. Hypotheses

It is hypothesised that the adaptive controllers combine the best properties of low and high LoHA controllers in terms of safety and conflicts. The following hypotheses concern the adaptive controllers compared to the conventional static controllers.

- The safety margins are smaller for manual driving and the low LoHA controller than for high, symmetric and asymmetric adaptive LoHA controllers, resulting in lower TLC values and more lane departures.
- The amount and size of conflicting torques are higher and bigger for the high LoHA controller than for the low, symmetric and asymmetric adaptive LoHA controllers.
- The subjective appreciation for both adaptive LoHA algorithms is higher than for the low and high LoHA controllers.

Furthermore it is hypothesised that the asymmetric algorithm will show stronger improvements than the symmetric algorithm in the following ways:

- The number and size of conflicting torques are higher and bigger for the symmetric adaptive controller than for the asymmetric adaptive controller.

III. Method

To test the hypotheses and probe the difference between adaptive and static LoHA controllers, a within subjects experimental design was used.

A. Apparatus

The experiment was performed in a fixed-based driving simulator at the department of Control and Simulation at the faculty of Aerospace Engineering of the Delft University of Technology. The visual representation was done with three projectors that covered a horizontal view of 180 degrees and a vertical view of 40 degrees. The actuation of the steering wheel was done with a MOOG FCS Ecol8000S actuator at 2500 Hz; steering wheel dampening (2 [Nms/rad]) and inertia (0.3 [Nms^2/rad]) are equal to those of earlier studies by Abbink[9]. The vehicle dynamics are simulated by a discrete time State-Space model. This setup and the vehicle dynamics are identical to earlier studies [3][43][44][33] and listed in (18). All data were recorded at a frequency of 100 Hz.

$$\begin{aligned} x(t+\Delta t) &= Ax(t) + Bu(t) \\ y(t) &= Cx(t) + Du(t) \end{aligned} \tag{17}$$

$$A = \begin{bmatrix} 0.8665 & -.03849 \\ 0.1313 & 0.9824 \end{bmatrix} \qquad B = \begin{bmatrix} -14.24 \\ 23.64 \end{bmatrix} \tag{18}$$
$$C = \begin{bmatrix} -0.292 & -0.1938 \\ -0.000577 & 0.02834 \end{bmatrix} \qquad D = \begin{bmatrix} 0 \\ 0 \end{bmatrix}$$

B. Participants

Fourteen participants voluntarily participated in the driving simulator experiment (9 male), without receiving financial compensation. All participants were or had been students at Delft University of Technology. The average age was 25.8 years old (SD = 1.8), and participants had their driving license for an average of 6.8 years (SD = 1.7). Of the subjects, eight had experience in driving with adaptive cruise control in the past year, all less than once a month. Six had driven with a Lane Keeping Assistance system in the past year, all less than once a month. Six participants had previous experience with driving simulators of which four had driven in the simulator that was used in this experiment.

C. Road Design

The road was designed to present a challenging environment in which drivers would benefit from haptic support. It consists of 16 curves with radii of 500 m that were equally divided between left and right turns. Curves have 150 m straight sections between them to prevent interference between subsequent curve exits and entries. Two different road widths (3.6 and 2.2m) were used as an independent factor to manipulate the TLC. Road widths were alternated twice to provide both width transitions: from wide to narrow and narrow to wide. Based on the road width the yaw rate uncertainty λ_{TLC} [23] was heuristically tuned at 0.2 deg/s to give the adaptive controllers a good response to the changes in road width.

The straights, curves, and two roadwidths result in four different road conditions which are analysed separately: *Narrow Straights* (NS), *Wide Straights* (WS), *Narrow Curves* (NC), and *Wide Curves* (WC) (Figure 7). Each of these unique road combination of curvature and road width was driven twice per trial. When including a run-in and -out section, the road had a total length of 7.3 kilometers.

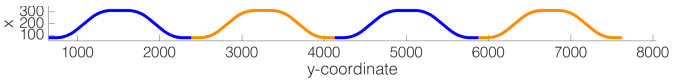

Fig. 7. Road curvature profile; narrow roads are red, wide roads are blue.

D. Controllers

In addition to manual driving, four different LoHA controllers were implemented and compared. For all trials the road, vehicle dynamics, LoHS, SoHF (Table II) and velocity (24 m/s) were identical.

- *Manual (M)*
  In the manual control condition in the LoHS and SoHF were set to 0, effectively disabling all forms of feedback or support. The inherent steering wheel stiffness was 0.0085 Nm/deg and acted around the steering wheel's neutral position (0 deg).
- *Low stiffness (L)*
  In this condition the Level of Haptic Authority was set to 0.0085 Nm/deg, the same as the inherent steering wheel

stiffness for manual driving but around the controller's desired steering wheel angle. It equals the lower LoHA boundary of the symmetrical and asymmetrical adaptive algorithms
- *High stiffness (H)*
  The high stiffness condition has a LoHA of 0.0255 Nm/deg and equals the upper LoHA boundary of the symmetrical and asymmetrical adaptive algorithms.
- *Symmetrical adaptive stiffness (S)*
  The Symmetrical adaptive LoHA determines the steering wheel stiffness by taking the lowest TLC value and determines the controller stiffness in the range of $\langle 0.0085$ - $0.0255 \rangle$ Nm/deg.
- *Asymmetrical adaptive stiffness (A)*
  The Asymmetrical adaptive LoHA determines the steering wheel stiffness by taking the TLC value in the direction of the human torque and determines the controller stiffness in the range of $\langle 0.0085$ - $0.0255 \rangle$ Nm/deg.

E. Procedure

For the experiment, participants were instructed to drive as they normally would and stay within the lane boundaries. After receiving task instructions and an opportunity for experiment related questions each participant drove two training routes, one manual and one with a high stiffness controller, to give experience with both extremes of the spectrum prior to the experiment. After two rounds of training the experimental conditions were presented in a randomised order to mitigate any learning effects. Between each of the testing conditions participants were asked to fill out two subjective questionnaires, the Van der Laan questionnaire [45] and the NASA Task Load Index [46]. Beyond the controller stiffness, all other experimental conditions such as: road profile, velocity, vehicle dynamics and controller parameters, were kept constant. If the vehicle was outside of the lane boundaries a high frequency disturbance, modelled by a 100 Hz sinewave, was applied on the steering wheel to alert the driver of the lane departure. The controller parameters are listed in Table II.

TABLE II
FDCA PARAMETER VALUES USED IN THE EXPERIMENT FOR THE STRENGTH OF HAPTIC FEEDBACK (SOHF), LEVEL OF HAPTIC SUPPORT (LOHS), AND LEVEL OF HAPTIC AUTHORITY (LOHA)

K_{y-SoHF}	0.3 [Nm/m]
$T_{\psi-SoHF}$	2.0 [Nm/rad]
λ_{LoHS}	80 [%]
K_{LoHA}	0.0085 - 0.0255 [Nm/deg]

F. Variables & Metrics

Driver support systems usually improve performance but also lead to conflict, affect workload and acceptance of the system. Hence metrics related to performance, conflicts, workload, and acceptance are analysed.

1) Performance and safety margins: It hypothesised the High and Adaptive LoHA controllers should improve lane keeping performance and safety margins, measured by:

- *Time Spent Out Of Lane [s]:* Due to the satisficing nature of human driving, only the task (lane keeping) failures are evaluated as a performance metric. The time spent out of lane captures frequency as well as intensity of the lane departures.
- *Mean Time To Lane Crossing Swath (TLC) [s]:* The TLC swath represents the situational criticality and thereby the safety [47], higher TLC's are the result of higher safety margins.
- *Mean 10 percentile of TLC [s]:* In light of satisficing driver behaviour the unsatisficing performances are mainly contained in the lower TLC percentiles, therefore the 10 percentile of TLC values is evaluated for improvements seperately [48].

2) Conflicts: It is hypothesised that the Low and Adaptive LoHA controllers should reduce conflicts between driver and controller, measured by:

- *Time spent in Conflict [s]:* Opposing torques from the driver and the controller can indicate conflicts in intentions. The time spent in conflict is evaluated, in this study the occurrence of a conflict is defined as opposing torques of the driver and HSC.
- *Mean Size of Conflicting Torques [Nm]:* In addition to the time spent in conflict, the size of the conflict tells something about the severity of the conflict and the physical workload.

3) Workload: It is hypothesised that adaptive algorithms will reduce driver workload as measured by:

- *NASA Task Load Index (TLX) [%]:* A subjective self-reported workload percentage. The unweighted version of the NASA TLX rating system was used called 'Raw TLX' [49]. The TLX rates six topics representing physical, mental and temporal demand [46]. Each item has to be graded with a score from 0 to 100. The workload is then determined by taking the average value.
- *Steering Reversal Rate (SRR)* $[s^{-1}]$: The steering reversal rate is determined by counting how many times the steering wheel is reversed with 2 degrees or more around a local minima and maxima, and is used as an objective measure for the workload [48].
- *Mean absolute Driver Torque* [Nm] The mean Absolute Driver Torque is the torque applied by the driver on the steering wheel over the total road section and is used as an objective measure for the driver's physical workload.

4) Subjective appreciation: It is hypothesised that the adaptive controllers, the asymmetric controller in particular, are subjectively preferred by drivers over the static controllers.

- *Van der Laan* To assess the acceptance of the systems the questionnaire from Van der Laan [45] is used, which plots each condition on a two dimensional plane spanned by usefulness scale and a satisfaction scale. The questionnaire consists of nine Likert items: Each item has to be graded with a score from -2 to + 2. The usefulness scale is determined with the sum of item 1, 3, 5, 7 and

9, divided by 5. The satisfactory scale is the sum of 2, 4, 6 and 8, divided by 4.

G. Statistical Analysis

The numerical results of each dependant measure were collected in a 14 x 5 matrix (14 participants and 5 conditions). This matrix was rank-transformed according to Conover and Iman [50] to account for violations of the assumption of normality associated with parametric tests. The rank-transformed matrix, consisting of ranks from 1 to 70, was submitted to a repeated measures ANOVA with the five conditions as within-subjects factor with an α-value of ($p<.05$). Bonferroni corrections were applied to the ten pairwise comparisons between the controller conditions. Seperate analyses were made for four distinct road conditions: Narrow Straights (NS), Wide Straights (WS), Narrow Curves (NC), and Wide Curves (WC).

IV. Results

The objective metrics are analysed separately for all four road conditions: *Narrow Straights* (NS), *Wide Straights* (WS), *Narrow Curves* (NC), and *Wide Curves* (WC).

All variables were analysed but not all are discussed in detail, particularly differences between HSC and manual driving are not discussed here as they are well described in literature [10]; the complete results of the statistical analyses can be found in Tables (V),(VI) and (VII).

TABLE III
RESULTS OF THE REPEATED MEASURES ANALYSIS OF VARIANCE FOR THE THREE MAIN PARAMTERS, RELATED TO THE HYPOTHESES. ALL PARAMTERS WERE SIGNIFICANTLY INFLUENCED BY THE CONTROLLERS ON NEARLY ALL ROAD SECTIONS.

		NS	WS	NC	WC
TLC	p	**4.95E-5**	**5.90E-7**	**2.91E-3**	**9.98E-4**
	F(4,56)	7.861	11.94	4.612	5.425
SoC	p	**4.29E-5**	**6.52E-5**	0.290	**7.57E-4**
	F(3,42)	10.21	9.700	1.307	6.924
SWR	p	**5.58E-14**	**3.95E-7**	**7.52E-11**	0.260
	F(4,56)	34.16	12.35	22.57	1.352

A. Mean trajectory performance

The mean performance over all participants is displayed in Figure (12). It is observed that the HCR cuts curves more aggressively than the participants, the high LoHA controller's mean trajectory is the closest to HCR indicating that a higher LoHA does indeed shift the trajectory towards the HCR. Consequently the CR's TLC is lower in curves than the mean of the drivers; on the wide roads the mean TLC is above the adaptivity threshold allowing for satisficing lane keeping, on narrow roads the mean TLC is well within the active range of the adaptive controllers. The LoHA follows the trends of the TLC, it can be observed that the symmetric controller is stiffer (i.e. has a higher LoHA) on average than the asymmetric controller. Steering angle disagreements between controller and driver mainly occur at curve entry and exit and are similar in size regardless of curve direction or road width, the resulting driver torques however are different for the different controllers and road width.

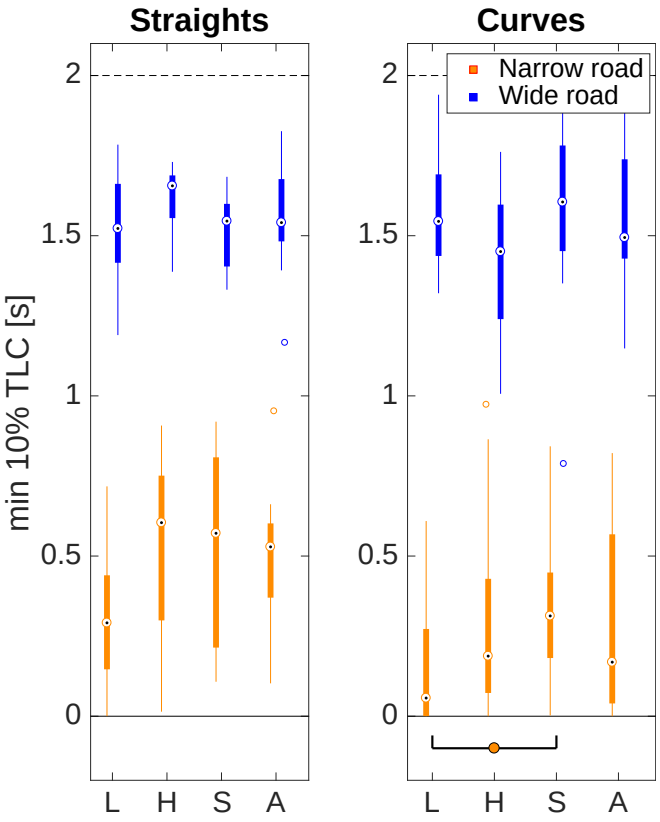

Fig. 8. Distribution of the lowest 10% TLC swath values for the four LoHA regimes in each road condition. All controller improved the lowest TLC values compared to manual driving but only one difference was found between controllers. Brackets indicate significant differences, ● → $p<.05$, ●● → $p<.01$, ●●● → $p<.001$.

B. Safety margins

As a measure for the safety margin the values of the TLC swath are analysed as a lower TLC is a lower safety margin [48]. Since we are especially interested in critical situations, the lowest 10% of values are assessed [39]. Effect sizes and significance are shown in Table III. The distributions of the controllers are shown in Figure 8. All other results and comparisons with manual driving can be found in Tables (V), (VI) and (VII). Although all controllers improve the lowest 10% of TLC values compared to manual driving, no differences were found between controllers except for narrow curves where the symmetric controller outperformed the low LoHA controller. This indicates the height of the LoHA does not have a significant influence on te safety margins, but haptic shared control does.

C. Conflicts

As a measure for the amount of conflict between driver and controller the average size of opposing torques was analysed, because manual driving does not involve a controller there are no conflicts and the manual condition is left out of the statistical analysis (Table III). The distributions are shown in Figure 9. The results show that the average conflict size was significantly affected by the LoHA regime on straights

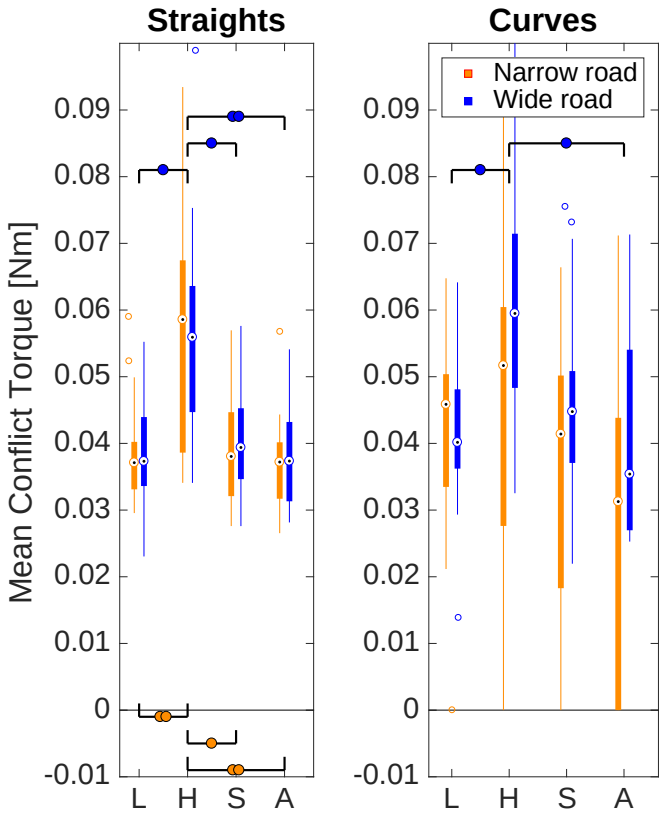

Fig. 9. Distribution of average conflict torques for the four LoHA regimes in each road condition. Brackets indicate significant differences, ● → p<.05, ●● → p<.01, ●●● → p<.001.

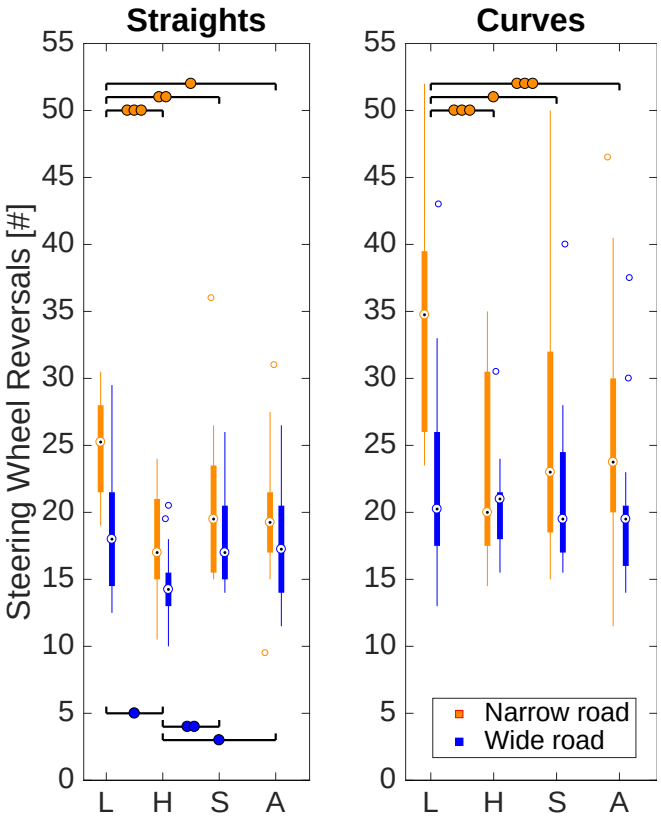

Fig. 10. Distribution of the number of steering wheel reversals. Brackets indicate significant differences, ● → p<.05, ●● → p<.01, ●●● → p<.001.

and in narrow curves. A Bonferroni corrected post-hoc comparison revealed that low LoHA, symmetric and asymmetric controllers result in a similar conflict size, lower than that of the high LoHA controller. The pairwise comparisons can be found in Table VII. In addition to conflict size the time spent in conflicts was also analysed. Especially in wide curves ($p<.05$, $F(3,42)=13.2$) the high LoHA controller resulted in a larger amount of time spent in conflict (M=30% SD=14%) than the other controllers (M=11% SD=8.8%), indicating high LoHA has a negative effect on both the size and occurrence of conflicts.

D. Workload

The number of Steering Wheel Reversals (SWR) indicates a significant difference in control activity, indicating workload, between controllers (Table III, Figure 10). In narrow road sections the number of SWR was significantly higher for low LoHA controller than for the high and adaptive controllers. On wide straights, the adaptive controllers instead behave like the low LoHA controller resulting in a significantly lower number of reversals for high LoHA compared to the other three controllers. Mean absolute driver torques, indicating physical workload, follow a different trend: the high LoHA controller results in higher driver torques than the other three controllers on all roads.

Subjectively however, contrasts with a Bonferroni adjustment did not reveal any significant differences in perceived workload between controllers in terms of TLX score. Compared to manual driving, all controllers were rated as to lower perceived workload.

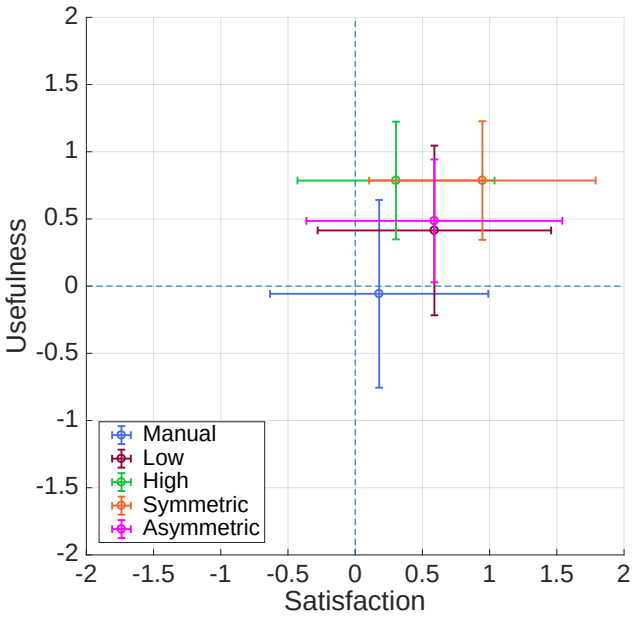

Fig. 11. Subjective rating of the controllers on the Van der Laan acceptance matrix [45].

E. Subjective rating

Lastly the subjective appreciation in terms of the perceived satisfaction and usefulness were assessed through the 'Van der Laan' questionnaire [45]. The results are shown in Figure 11. All subjective data was normally distributed and spherical, a one-way repeated measures ANOVA revealed there were no significant difference between the controllers. Compared to manual driving however, high LoHA and symmetric adaptive LoHA were rated as significantly more useful.

V. Discussion

The aim of the study was to compare adaptive LoHA algorithms to static tunings of LoHA. More specifically it was hypothesized that compared to manual control, a high static LoHA leads to improved safety margins with increased conflict torques and that both adaptive LoHA systems lead to similar safety margin improvements with smaller conflict torques. Furthermore the symmetric adaptive and asymmetric adaptive controllers controllers are compared, the asymmetric adaptive controller is hypothesised to have smaller conflict torques than the symmetric adaptive controller but with similar safety margins.

A. Main results

1) Safety margins: In the lowest 10% of TLC values, no significant differences were found between the controllers, not even between the high and low stiffness controllers. A possible explanation for the lacking difference between the low and high LoHA controller can be sought in de differences between the HCR and mean driver performance. In the study, drivers had a relatively high mean TLC compared to what was expected based on the TLC of the HCR. Curves were cut more aggressively by the HCR than by the drivers resulting in lower TLC values when following the HCR; positively the LoHA also didn't affect the TLC negatively despite the more critical HCR trajectory. To find differences between the controllers the HCR should have been more conservative in its curve cutting. The quality of the HCR will be further discussed in section V-B.

2) Conflicts: Conflicts can be evaluated in terms of how frequently they occur and their magnitude. It should be noted first of all that the amount of data points for conflict for narrow curves is relatively low, driver spent less than 1% of their time on these sections in conflict with the controllers (M=0.66% SD=0.55%). In contrast, on straight sections it is relatively high (M=68.1% SD=9.44%) since any steering movement away from the road centre or overcompensation is considered a conflict with the controller which follows the dead centre of the road.

It is observed that the LoHA affects the time spent in conflict on wide curves, which is the road section where the HCR and manual trajectories lie furthest apart. Here it becomes apparent a stiffer LoHA restricts the envelope of conflict free trajectories and that a stiffer LoHA results in drivers having to produce opposing torques to follow their preferred trajectory outside of this envelope. This is a direct result of the design choice of keeping the required torque to follow the HCR rather than the required steering angle independent of LoHA: As LoHA increases the torque to follow the HCR remains constant but consequently the controller's steering offset (i.e. the conflict free steering range) as governed by the LoHS is proportionally reduced; as the LoHA approaches infinity the steering wheel will end up at the controller's desired steering wheel angle, regardless of the LoHS.

The size of conflicts is also significantly affected: the low, symmetric and asymmetric LoHA controllers result in lower conflicts than high LoHA on straights and wide curvatures thus proving adaptive LoHA, like low LoHA, is an effective way to achiever lower conflicts than with high LoHA controllers.

3) Workload: When observing the three workload related metrics: steering wheel reversals, driver torque, and perceived workload; three different messages are communicated through the metrics: the physical component of workload represented by the mean driver torque goes up with higher LoHA. Meanwhile the number of steering wheel reversals goes down, indicating a lower workload, and subjectively no difference was perceived. So what is happening?

First of all a higher mean driver torque is a logical result of a higher LoHA, despite the FDCA controller being designed such that drivers need the same amount of torque to follow the HCR regardless of the LoHA. A significant percentage of time was spent in conflict with the controller (M=38.1%, SD=7.40%) and the size of conflicts is significantly effected by the LoHA, these torques end up contributing to the total mean driver torque.

Second, the steering wheel reversal rate; a stiffer steering wheel due to higher LoHA restricts overshooting steering corrections. Since steering reversals are measured as an opposing steering movement of over two degrees [48], it makes sense that high LoHA leads to a reduction. On wide roads this means restricted satisficing behaviour but drivers also benefit from a reduction in steering wheel reversals, especially on narrow roads [2][10]. High LoHA has positive and negative effects on different aspects of workload compared to the low LoHA controllers, but the adaptive controllers seem to combine the best of both worlds: a reduced number of steering wheel reversals and a lower driver torque. apparently corrective steering reversals occur most while at low TLC and are reduced by the adaptive algorithms without affecting the driver torque at road sections with high LoHA.

The self-reported perceived workload offers no decisive results in what drivers value more and under which conditions. But with two out of three metric in favour of adaptive algorithms and one neutral it can be concluded the workload is reduced by the adaptive algorithm.

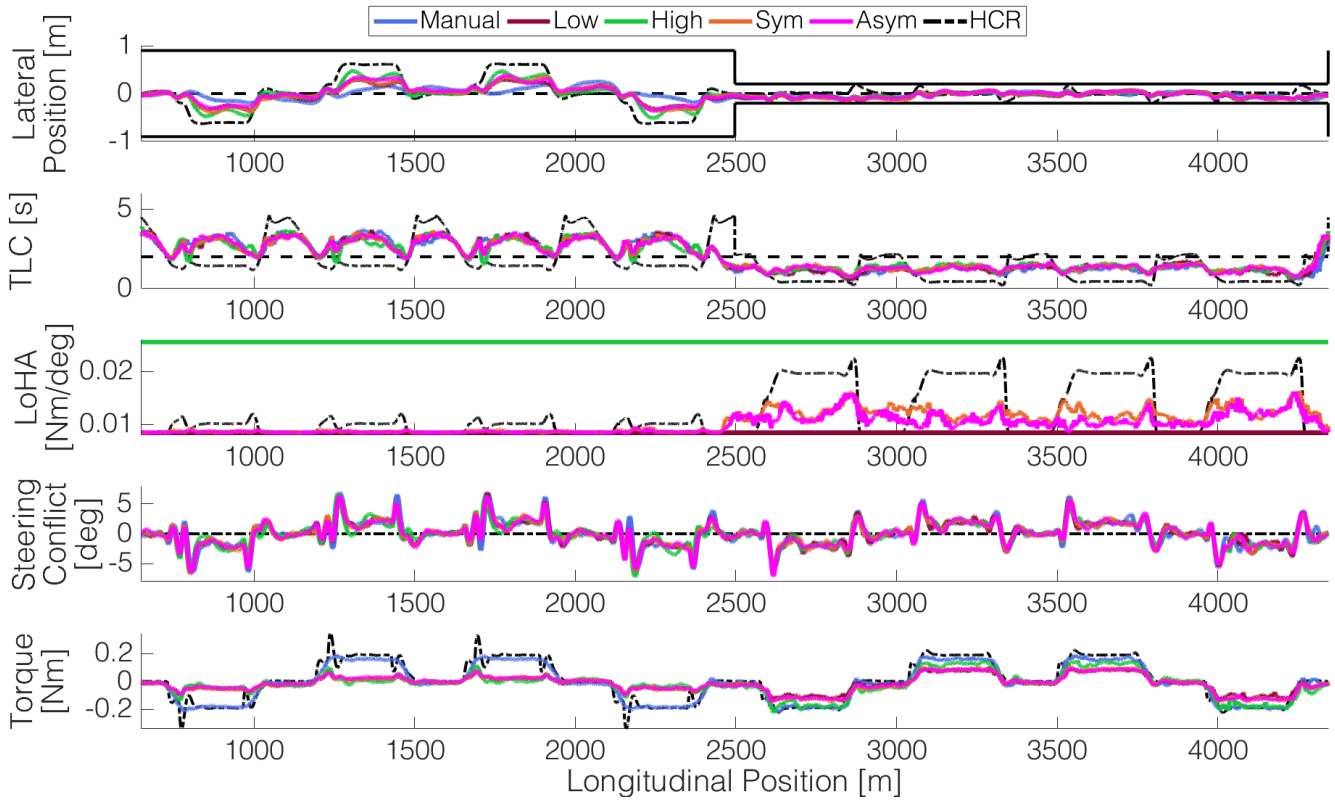

Fig. 12. Time traces for the mean performanc over all subjects alongside the theoretical HCR performance. Illustrating the behaviour in left and right curves, and on straights for both narrow and wide roads It is observed that on average the HCR cuts curves more aggressively than the participants. On the wide road the TLC and LoHA means are above the adaptive threshold allowing for satisficing behaviour, on the narrow road the mean performance falls well in the adaptive range of TLC values, resulting in stiffer symmetric and asymmetric adaptive controllers.

4) Subjective Appreciation: The results of the Van der Laan questionnaire show positive trends for the adaptive controllers but no significant differences between controllers. The utilised Likert scale has a rather small discrete range resulting in quite a large variability across metrics and difficulty giving distinct scores for controllers. all controllers were rated positively in terms of usefulness and satisfaction. During the experiment two global categories of drivers were observed based on their verbal comments: a group that disliked the HCR, reported conflicts and would generally give worse subjective ratings at higher LoHA. And a group that was comfortable with the support and rate the controllers the exact opposite way.
LoHA is effective at managing the size of conflicts but the occurrence of conflicts is almost completely dictated by the match between the driver and the HCR; this underlines the variability between humans and the importance of personalised trajectories [16][33].

B. Quality of the Human Compatible Reference

A single HCR was implemented as basis for the sared controller. In a seperate analysis we compared the illustrated these trajectories differed for a significant percentage of time. The average conflict of an individual driver with the HCR was the following: Narrow Straights= 66% , Wide Straights=70%, Narrow Curves=0.66%, Wide Curves=16%. On straight sections this percentage does not indicate much since any deviation from driving in the middle will result in a conflict. In wide corners however, drivers still spent an average 16% of the time steering in conflict with the controller despite the LoHS being set at only 75%. This is caused by the agressive curve cutting of the HCR in wide turns.

The road design is the most probable cause of a mismatch: the parameters of the lookahead controller were taken from the 'mean of all subjects' controller of [33] for right curves. The road in this study however, was designed with different parameters: Scholten's road used a roadwidth of 3.6m and clothoidal curves with a radius of 300m, where this study used roadwidths of 3.6 and 2.2m and tangent curves with a radius of 500m. Since wider curves have longer arc lengths with tangent points that lie further away and narrow roads have a smaller margin for cutting or overshooting curves it is probable the HCR parameters would be different.

Curve negotiation is also very dependent on the personal driving style [51], Scholtens' test group may have had a significantly different driving style but this is impossible to validate post-hoc. Either way, both explanations indicate that

for the HCR of future FDCA studies, the controller parameters should be carefully tuned to the specific road conditions and participants as per Scholtens' method. Although the LoHA itself is unaffected by the HCR, it should result in more agreeable steering angles.

C. Yaw variability

The shape of the TLC swath used in this study is largely defined by the yaw uncertainty (λ_{TLC}) as defined in Boer's[23] method. λ_{TLC} was heuristically tuned at 0.2 deg/s for good controller responses to the given roadwidths at a two second threshold, for the HCR this also resulted in TLC values well in the adaptive region (Figure 12). After analysis of the recorded data over all conditions the actual mean yaw deviation with respect to the road curvature is found to be roughly three and a half times higher (M=0.6901 deg/s, SD=0.0553) than λ_{TLC}. The yaw rate was more variable than expected. meaning that the simulated TLC swath was an over-estimation compared to calculations based on the actual yaw variability.

The results of the adaptive algorithms may have suffered from this over-estimation as they respond relatively later and weaker than they would have with the actual yaw variability. Future research should explore basing the λ_{TLC} on live measurements the actual current yaw variability, for example through a moving mean, this would give a closer match with the individual driver and the current road. The resulting lower TLC values, based on observations in this study, would increase the sensitivity of the adaptive controller.

D. Symmetric vs Asymmetric Stiffness

For none of the dependent variables at any of these sections there was a significant difference between the symmetric and asymmetric adaptive LoHA (Table VII). The question arises if the algorithms resulted in significantly different LoHA values to begin with? A Wilcoxon non-parametric test was used to compare the two controllers, results are found in Table IV: on narrow straights and curves the asymmetric controller resulted in a lower TLC than the symmetric controller.

It has also been shown that LoHA significantly affects parameters such is the size of conflicts or the number of steering wheel reversals. With both effects observed, why do the symmetric and asymmetric controllers not manifest themselves in different conflict sizes or steering wheel reversals? Although the difference in LoHA is significant, the percentual difference is only about 10%, too subtle to translate in further effects. This difference is expected to grow as the TLC values lie deeper into the active zone of the adaptive algorithms as this increases te difference between the a adaptive LoHA and its lower boundary.

In a future study the TLC can be placed further in the adaptive region by widening the TLC swath by means of λ_{TLC} as discussed by the previous section, or by raising the adaptive threshold above two seconds, stretching up the adaptive zone. Placing the upper and lower LoHA limits are further apart can also be used to increase the absolute difference between the symmetric and asymmetric controller. In this study the upper LoHA limit in this study was tuned on the subjective appreciation of the high LoHA controller, yet a high stiffness in an adaptive controller might be appreciated even when it is disliked in a static LoHA controller because it is only applied in low TLC situations. Neuromuscular admittance based tuning [15, 14] for relax and position tasks may be a good basis for tuning the LoHA limits.

TABLE IV
COMPARISON OF THE RESULTING LOHA VALUES OF THE SYMMETRIC AND ASYMMETRIC CONTROLLER, BONFERRONI CORRECTED ($p < .0125$ SIGNIFICANCE THRESHOLD). ON NARROW ROAD SECTIONS THE CONTROLLERS ARE SIGNIFICANTLY DIFFERENT.

		NS	WS	NC	WC
Symmetric	M	0.0117	0.00867	0.01241	0.00871
	(SD)	(0.0012)	(0.00008)	(0.00122)	(0.00033)
Asymmetric	M	0.0107	0.00862	0.01147	0.00864
	(SD)	(0.0006)	(0.00012)	(0.00130)	(0.00014)
	p	**0.005**	0.041	**0.001**	0.300
	Z	-2.794	-2.040	-3.296	-1.036

E. Feedback controller

While the LoHA was made adaptable the remaining FDCA control parameters, LoHS and SoHF, had a constant value tuning for the entire road. Both the narrow and wide road sections were driven with the same controller parameters while it could be argued at least the feedback controller should have scaled with the roadwidth: the same deviation from the HCR results in different safety margins but the feedback gains did not reflect this.

F. Inclusion of driver state parameters

The current adaptive TLC controllers factor in many environmental and performance parameters but do not include measurements of the driver's mental state. This would be a promising field for future research: mental state greatly influences the capabilities of the driver [52] and the amount of support and correction they need. Driver mental state is difficult to assess and many methods are intrusive to the driving task [53]. A promising solution is proposed by Azimet et al. [54] who used an eye-tracker with a fuzzy-expert system to assess drowsiness and attention in driving, such data could be helpful when determining the amount of support or if an intervention should be performed by the controller. In adaptive supervisory control Gartenberg [55] has already applied eye-tracker based methods with success.

G. Implications for real world driving

In the simulator study the driving task was constrained to fixed speed lane keeping without other traffic or intersections

and at six minutes the experiment was rather short compared to real driving; so how do the results translate to real world driving? Although only one velocity was investigated, literature has shown that TLC scales well with velocity and drivers shows similar behaviour at equal TLC distances, regardless of the velocity [29]. Of course driver behaviour in simulators is different from regular driving, people have a different, lower, perception of risk [56] so the magnitude of the TLC thresholds and yaw uncertainty that lie at the basis of the adaptive algorithm will need to be re-evaluated for real driving.

VI. Conclusion

The goal of this study was to develop and evaluate an adaptive LoHA algorithm based on TLC that can achieve an increase in safety margins similar to a static high stiffness controller without the drawbacks of high conflicts and driver dissatisfaction. The algorithms were objectively and subjectively evaluated on a simulator track with two distinct road widths to emulate scenarios with different safety margins and compared to manual driving as well as driving with a low and high static LoHA. It was hypothesised that the adaptive algorithms would increase the safety margins compared to low static LoHA, reduce the conflict size compared to high static LoHA and reduce workload measured by torque, steering wheel reversals and subjective reports.

Adaptive LoHA controllers effectively reduces the size of conflicts compared to a high LoHA controller and driver workload compared to a low LoHA controller.
However, no effect of LoHA on the safety margins was found nor was there a difference between the symmetric and asymmetric adaptive controllers in terms of steering behaviour.

Future studies should investigate the effects of the adaptive controllers on safety margins when the TLC is deeper in the adaptive region, this can be achieved by picking a higher upper LoHA limit, heightening the adaptivity threshold and widening the TLC swath. But even without an effect on the safety margins, these results show that adapting the LoHA to the environment is a better than static LoHA at giving driver support when needed.

References

[1] D. A. Abbink, M. Mulder, and E. R. Boer, "Haptic shared control: Smoothly shifting control authority?" *Cognition, Technology and Work*, vol. 14, no. 1, pp. 19–28, 2012.

[2] F. O. Flemisch, J. Kelsch, C. Loper, A. Schieben, J. Schindler, and H. Matthias, "Cooperative Control and Active Interfaces for Vehicle Assistance and Automation," *FISITA World Automotive Congress*, no. 2, pp. 301–310, 2008.

[3] S. M. Petermeijer, D. A. Abbink, and J. C. de Winter, "Should Drivers Be Operating Within an Automation-Free Bandwidth? Evaluating Haptic Steering Support Systems With Different Levels of Authority," *Human Factors: The Journal of the Human Factors and Ergonomics Society*, vol. 57, pp. 5–20, 2014. [Online]. Available: http://hfs.sagepub.com/content/57/1/5.hort

[4] B. A. C. Forsyth and K. E. MacLean, "Predictive Haptic Guidance: Intelligent User Assistance for the Control of Dynamic Tasks," *IEEE Transactions on Visualization and Computer Graphics*, vol. 12, no. 1, pp. 103–113, 2006.

[5] P. G. Griffiths and B. Gillespie, "Sharing control between humans and automation using haptic interface: primary and secondary task performance benefits." *Human factors*, vol. 47, no. 3, pp. 574–90, 2005. [Online]. Available: http://www.ncbi.nlm.nih.gov/pubmed/16435698

[6] M. Mulder, D. A. Abbink, and E. R. Boer, "The effect of haptic guidance on curve negotiation behavior of young, experienced drivers," *Conference Proceedings - IEEE International Conference on Systems, Man and Cybernetics*, pp. 804–809, 2008.

[7] M. Steele and R. Gillespie, "Shared Control between human and machine: using a haptic steering wheel to aid in land vehicle guidance," in *PROCEEDINGS of the HUMAN FACTORS AND ERGONOMICS SOCIETY 45th ANNUAL MEETING*, vol. 45, no. 1992, 2001, pp. 1671–1675.

[8] T. Inagaki, "Adaptive Automation: Sharing and Trading of Control," *Handbook of Cognitive Task Design*, pp. 147–169, 2003. [Online]. Available: http://css.risk.tsukuba.ac.jp/pdf/tutorial07.pdf

[9] D. A. Abbink and M. Mulder, "Neuromuscular Analysis as a Guideline in designing Shared Control," pp. 499–517, 2010.

[10] J. C. de Winter and D. Dodou, "Preparing drivers for dangerous situations: A critical reflection on continuous shared control," in *Conference Proceedings - IEEE International Conference on Systems, Man and Cybernetics*, 2011, pp. 1050–1056.

[11] J. Smisek, W. Mugge, J. B. J. Smeets, M. M. Van Paassen, and A. Schiele, "Adapting haptic guidance authority based on user grip," *Conference Proceedings - IEEE International Conference on Systems, Man and Cybernetics*, vol. 2014-Janua, no. January, pp. 1516–1521, 2014.

[12] T. M. Lam, M. Mulder, and M. M. Van Paassen, "Haptic interface in UAV tele-operation using force-stiffness feedback," *Conference Proceedings - IEEE International Conference on Systems, Man and Cybernetics*, no. October, pp. 835–840, 2009.

[13] D. A. Abbink and M. Mulder, "Exploring the Dimensions of Haptic Feedback Support in Manual Control," *Journal of Computing and Information Science in Engineering*, vol. 9, no. March 2009, p. 011006, 2009.

[14] J. Smisek, S. Member, E. Sunil, M. M. V. Paassen, S. Member, D. A. Abbink, and M. Mulder, "Neuromuscular-System-Based Tuning of a Haptic Shared Control Interface for UAV Teleoperation," pp. 1–13, 2016.

[15] D. A. Abbink, D. Cleij, M. Mulder, and M. M. Van Paassen, "The importance of including knowledge of

neuromuscular behaviour in haptic shared control," *Conference Proceedings - IEEE International Conference on Systems, Man and Cybernetics*, pp. 3350–3355, 2012.

[16] R. P. Boink, M. M. Van Paassen, M. Mulder, and D. A. Abbink, "Understanding and reducing conflicts between driver and haptic shared control," *Conference Proceedings - IEEE International Conference on Systems, Man and Cybernetics*, vol. 2014-Janua, no. January, pp. 1510–1515, 2014.

[17] F. Mars, M. Deroo, and J. M. Hoc, "Analysis of human-machine cooperation when driving with different degrees of haptic shared control," *IEEE Transactions on Haptics*, vol. 7, no. 3, pp. 324–333, 2014.

[18] D. Toffin, G. Reymond, A. Kemeny, and J. Droulez, "Role of steering wheel feedback on driver performance : driving simulator and modeling analysis," vol. 3114, no. February, 2007. [Online]. Available: http://dx.doi.org/10.1080/00423110601058874

[19] M. Mulder, D. A. Abbink, and E. R. Boer, "Sharing Control With Haptics Seamless Driver Support From Manual to Automatic Control," *Human Factors: The Journal of the Human Factors and Ergonomics Society*, vol. 54, no. 5, pp. 786–798, 2012. [Online]. Available: http://hfs.sagepub.com/content/54/5/786{\%}5Cnhttp://hfs.sagepub.com/content/54/5/786.full.pdf{\%}5Cnhttp://hfs.sagepub.com/content/54/5/786.short{\%}5Cnhttp://www.ncbi.nlm.nih.gov/pubmed/23156623

[20] R. Parasuraman and V. Riley, "Humans and Automation: Use, Misuse, Disuse, Abuse," *Human Factors: The Journal of the Human Factors and Ergonomics Society*, vol. 39, no. 2, pp. 230–253, 1997. [Online]. Available: http://hfs.sagepub.com/cgi/doi/10.1518/001872097778543886

[21] F. O. Flemisch, J. Kelsch, C. Löper, A. Schieben, and J. Schindler, "Automation spectrum , inner/outer compatibility and other potentially useful human factors concepts for assistance and automation," *Human Factors for Assistance and Automation*, no. 2008, pp. 1–16, 2008.

[22] M. A. Goodrich, W. C. Stirling, and L. R. Bolr, "Satisficing revisited," *Minds and Machines*, vol. 10, no. 1, pp. 79–110, 2000.

[23] E. R. Boer, "Satisficing Curve Negotiation: Explaining Drivers' Situated Lateral Position Variability," *IFAC-PapersOnLine*, vol. 49, no. 19, pp. 183–188, 2016. [Online]. Available: http://dx.doi.org/10.1016/j.ifacol.2016.10.483

[24] M. Mulder, D. A. Abbink, E. R. Boer, and M. M. Van Paassen, "Human-centered Steer-by-Wire design: Steering wheel dynamics should be task dependent," *Conference Proceedings - IEEE International Conference on Systems, Man and Cybernetics*, pp. 3015–3019, 2012.

[25] C. Passenberg, A. Glaser, and A. Peer, "Exploring the design space of haptic assistants: The assistance policy module," *IEEE Transactions on Haptics*, vol. 6, no. 4, pp. 440–452, 2013.

[26] K. Suzuki and H. Jansson, "An analysis of driver's steering behaviour during auditory or haptic warnings for the designing of lane departure warning system," *JSAE Review*, vol. 24, no. 1, pp. 65–70, 2003.

[27] J. J. Gibson and L. E. Crooks, "A Theoretical Field-Analysis of Automobile-Driving," *The American Journal of Psychology*, vol. 51, no. 3, pp. 453–471, 1938. [Online]. Available: http://www.jstor.org/stable/1416145

[28] V. Papakostopoulos, N. Marmaras, and D. Nathanael, "The field of safe travel revisited: interpreting driving behaviour performance through a holistic approach," *Transport Reviews*, vol. 37, no. 6, pp. 695–714, 2017. [Online]. Available: http://dx.doi.org/10.1080/01441647.2017.1289992

[29] H. Godthelp, "The limits of path error-neglecting in straight lane driving," *Ergonomics*, vol. 31, no. 4, pp. 609–619, 1988.

[30] D. W. J. Van Der Wiel, M. M. Van Paassen, M. Mulder, and D. A. Abbink, "Driver Adaptation to Driving Speed and Road Width: Exploring Parameters for Designing Adaptive Haptic Shared Control," *Proceedings - 2015 IEEE International Conference on Systems, Man, and Cybernetics, SMC 2015*, pp. 3060–3065, 2015.

[31] M. M. V. Paassen, R. Boink, D. A. Abbink, M. Mulder, and M. Mulder, "Four design choices in Haptic shared control," in *Advances in Aviation Psychology, Volume 2: Using Scientific Methods to Address Practical Human Factors Needs*, 2017, ch. 12, pp. 237 – 254. [Online]. Available: https://books.google.nl/books?hl=nl{\&}lr={\&}id=8iolDwAAQBAJ{\&}oi=fnd{\&}pg=PA237{\&}dq=Four+design+choices+for+haptic+shared+control,{\&}ots=3dIY4HZ0Ex{\&}sig=xSM77hpZWJkiQy2c5BfBX2WEBGY{\#}v=onepage{\&}q=Fourdesignchoicesforhapticsharedcontrol{\%}2C{\&}f=false

[32] P. Wyzen, M. M. Van Paassen, and D. A. Abbink, "Separating Haptic Guidance and Support Signals : a Solution for Human-Machine Cooperation ? (MSc thesis)," Tech. Rep., 2017.

[33] W. M. Scholtens, S. Barendswaard, D. A. Abbink, and S. Member, "Reducing conflicts in Haptic Shared Control during curve negotiation (MSc thesis)," Tech. Rep. January, 2018.

[34] L. Saleh, P. Chevrel, F. Mars, J. F. Lafay, and F. Claveau, *Human-like cybernetic driver model for lane keeping*. IFAC, 2011, vol. 18, no. PART 1. [Online]. Available: http://dx.doi.org/10.3182/20110828-6-IT-1002.02349

[35] E. R. Boer, "Tangent point oriented curve negotiation," *Proceedings of the 1996 IEEE Intelligent Vehicles Symposium*, no. 617, pp. 7–12, 1996. [Online]. Available: http://ieeexplore.ieee.org/xpls/abs{_}all.jsp?arnumber=566341

[36] S. Butterworth, "On the theory of filter amplifiers," pp. 536–541, 1930.

[37] F. C. T. Van Der Helm, A. C. Schouten, E. De Vlugt, and G. G. Brouwn, "Identification of intrinsic and reflexive components of human arm dynamics during postural control," *Journal of Neuroscience Methods*, vol. 119, no. 1, pp. 1–14, 2002.

[38] M. Kawato, "Internal Models for Motor Control and Trajectory Planning." pp. 718–727, 1999. [Online]. Avail-

able: http://dx.doi.org/10.1016/S0959-4388(99)00028-8

[39] H. Godthelp, P. Milgram, and G. J. Blaauw, "The development of a time-related measure to describe driving strategy," *Human Factors*, vol. 26, no. 3, pp. 257–268, 1984.

[40] T. J. Triggs and W. G. Harris, "Reaction Time of Drivers to Road Stimuli," *Medicinski Pregled*, vol. 62, no. June 1982, pp. 114–9, 1982. [Online]. Available: http://www.monash.edu.au/miri/research/reports/other/hfr12.pdf

[41] H. Li, N. Sarter, C. D. Wickens, and A. Sebok, "Supporting Human-Automation Collaboration Through Dynamic Function Allocation: The Case of Space Teleoperation," *Proceedings of the Human Factors and Ergonomics Society Annual Meeting*, vol. 57, no. 1, pp. 359–363, 2013. [Online]. Available: http://pro.sagepub.com/content/57/1/359.abstract

[42] S. K. Card, T. P. Moran, and A. Newell, *The psychology of human-computer interaction*, 1983. [Online]. Available: https://www.worldcat.org/oclc/9042220

[43] T. Melman, J. C. de Winter, and D. A. Abbink, "Does haptic steering guidance instigate speeding? A driving simulator study into causes and remedies," *Accident Analysis and Prevention*, vol. 98, pp. 372–387, 2017. [Online]. Available: http://dx.doi.org/10.1016/j.aap.2016.10.016

[44] S. Oudshoorn, S. Kolekar, and D. Abbink, "Design of Criticality-Based Haptic Steering Guidance for Human Like Adaptation to Different Lane Keeping Tasks (MSc thesis)," Tech. Rep. July, 2017.

[45] J. Van Der Laan, A. Heino, and D. De Waard, "A simple procedure for the assessment of acceptance of advance transport telematics," *Transportm Res.-C*, vol. 5, pp. 1–10, 1997.

[46] S. G. Hart and L. E. Sta, "Development of NASA-TLX (Task Load Index): Results of Empirical and Theoretical Research," *Human mental workload*, 1988.

[47] W. Van Winsum, K. A. Brookhuis, and D. De Waard, "A comparison of different ways to approximate time-to-line crossing (TLC) during car driving," *Accident Analysis and Prevention*, vol. 32, no. 1, pp. 47–56, 2000.

[48] E. Johansson, J. Engström, C. Cherri, E. Nodari, A. Toffetti, R. Schindhelm, and C. Gelau, "Review of existing techniques and metrics for IVIS and ADAS assessment," *Aide Project*, no. March, pp. 1–93, 2004.

[49] S. G. Hart, "Nasa-Task Load Index (NASA-TLX); 20 Years Later," *Proceedings of the Human Factors and Ergonomics Society Annual Meeting*, vol. 50, no. 9, pp. 904–908, 2006. [Online]. Available: http://journals.sagepub.com/doi/10.1177/154193120605000909

[50] W. J. Conover and R. L. Iman, "Rank Transformations as a Bridge Between Parametric and Nonparametric Statistics Author (s): W . J . Conover and Ronald L . Iman Published by : Taylor & Francis , Ltd . on behalf of the American Statistical Association Stable URL : http://www.jstor.org/," *The American Statistician*, vol. 35, no. 3, pp. 124–129, 1981.

[51] P. Spacek, "Track Behavior in Curve Areas: Attempt at Typology," *Journal of Transportation Engineering*, vol. 131, no. 9, pp. 669–676, 2005. [Online]. Available: http://www.scopus.com/inward/record.url?eid=2-s2.0-24944522100{\%}7B{\&}{\%}7DpartnerID=tZOtx3y1

[52] J. Nilsson, N. Strand, P. Falcone, and J. Vinter, "Driver performance in the presence of adaptive cruise control related failures: Implications for safety analysis and fault tolerance," *2013 43rd Annual IEEE/IFIP Conference on Dependable Systems and Networks Workshop (DSN-W)*, pp. 1–10, 2013. [Online]. Available: http://ieeexplore.ieee.org/document/6615531/

[53] R. J. Lysaght, S. G. Hill, a. O. Dick, B. D. Plamondon, P. M. Linton, W. W. Wierwille, a. L. Zaklad, a. C. Bittner Jr, and R. J. Wherry, "Operator workload: Comprehensive review and evaluation of operator workload methodologies," *United States Army Research Institute for the Behavioral Sciences, Technical Report*, vol. 851, pp. 903–986, 1989.

[54] T. Azim, M. A. Jaffar, and A. M. Mirza, "Fully automated real time fatigue detection of drivers through Fuzzy Expert Systems," *Applied Soft Computing Journal*, vol. 18, no. MAY, pp. 25–38, 2014.

[55] D. Gartenberg, L. A. Breslow, J. Park, J. M. McCurry, and J. G. Trafton, "Adaptive automation and cue invocation: The Effect of Cue Timing on Operator Error," *Proceedings of the SIGCHI Conference on Human Factors in Computing Systems - CHI '13*, pp. 3121–3130, 2013. [Online]. Available: http://dl.acm.org/citation.cfm?id=2470654.2466426

[56] J. C. de Winter, P. van Leeuwen, and R. Happee, *Video-BasedAdvantages and Disadvantages of Driving Simulators: A Discussion.*, 2012. [Online]. Available: http://citeseerx.ist.psu.edu/viewdoc/download?doi=10.1.1.388.1603{\&}rep=rep1{\&}type=pdf{\#}page=75

TABLE V
ANALYSIS OF VARIANCE ON STRAIGHTS. ALL DATA WAS RANK TRANSFORMED ACCORDING TO CONOVER & IRMAN (1981) [50] BEFORE BEING RUN THROUGH A RANOVA

	Narrow Straights							Wide Straights						
Controller	M	L	H	S	A			M	L	H	S	A		
Variable	M (SD)	M (SD)	M (SD)	M (SD)	M (SD)	pValue	F(4,56)	M (SD)	M (SD)	M (SD)	M (SD)	M (SD)	pValue	F(4,56)
Time out of bounds [%]	7.78 (5.546)	4.663 (3.115)	2.305 (2.681)	2.822 (3.63)	2.834 (3.461)	0.000128	7.063319	0.001 (0.005)	0.002 (0.006)	0 (0)	0.007 (0.023)	0.002 (0.006)	0.47843	0.88678
Time to Lane Crossing mean swath value [s]	1.241 (0.157)	1.383 (0.121)	1.467 (0.169)	1.416 (0.149)	1.415 (0.121)	2.73E-05	8.369726	2.777 (0.112)	2.87 (0.143)	2.918 (0.179)	2.851 (0.1)	2.837 (0.134)	0.018797	3.247759
Time to Lane Crossing mean minimum 10% [s]	0.184 (0.185)	0.309 (0.224)	0.536 (0.284)	0.531 (0.317)	0.476 (0.233)	4.94E-05	7.860679	1.4 (0.109)	1.532 (0.168)	1.621 (0.093)	1.519 (0.109)	1.566 (0.179)	5.9E-07	11.94244
Steering Wheel Reversals [#]	29.929 (4.228)	24.893 (4.166)	17.321 (3.871)	20.607 (5.735)	20.107 (5.439)	5.58E-14	34.16084	22.25 (4.874)	18.679 (4.874)	14.607 (3.157)	18.107 (3.748)	17.821 (4.272)	3.95E-07	12.34692
Average driver torque [Nm]	0.03 (0.006)	0.028 (0.005)	0.047 (0.011)	0.03 (0.007)	0.028 (0.006)	5.74E-09	16.98629	0.025 (0.004)	0.028 (0.011)	0.042 (0.012)	0.027 (0.009)	0.023 (0.009)	3.2E-06	10.30695
						pValue	F(3,42)						pValue	F(3,42)
Time in conflict [%]		60.835 (6.494)	67.338 (10.582)	69.128 (8.083)	66.228 (10.564)	0.003997	5.215609		72.712 (8.699)	73.787 (9.612)	67.585 (9.965)	67.305 (11.509)	0.022096	3.586192
Average size of conflict [Nm]		0.039 (0.009)	0.056 (0.018)	0.039 (0.008)	0.037 (0.008)	4.29E-05	10.20743		0.039 (0.008)	0.057 (0.018)	0.04 (0.008)	0.038 (0.008)	6.52E-05	9.700262

TABLE VI
ANALYSIS OF VARIANCE IN CURVES. ALL DATA WAS RANK TRANSFORMED ACCORDING TO CONOVER & IRMAN (1981) [50] BEFORE BEING RUN THROUGH A RANOVA

	Narrow Curves							Wide Curves						
Controller	M	L	H	S	A			M	L	H	S	A		
Variable	M (SD)	M (SD)	M (SD)	M (SD)	M (SD)	pValue	F(4,56)	M (SD)	M (SD)	M (SD)	M (SD)	M (SD)	pValue	F(4,56)
Time out of bounds [%]	7.666 (4.082)	8.919 (6.013)	6.432 (5.445)	4.143 (3.219)	5.889 (4.988)	0.000871	5.529963	0 (0)	0 (0)	0.063 (0.234)	0.112 (0.419)	0.069 (0.252)	0.423034	0.986669
Time to Lane Crossing mean swath value [s]	1.158 (0.134)	1.137 (0.198)	1.247 (0.19)	1.258 (0.152)	1.207 (0.19)	0.003446	4.486137	2.917 (0.123)	2.801 (0.19)	2.693 (0.211)	2.763 (0.25)	2.786 (0.231)	0.000102	7.253436
Time to Lane Crossing mean minimum 10% [s]	0.168 (0.176)	0.165 (0.227)	0.314 (0.329)	0.355 (0.264)	0.287 (0.299)	0.002911	4.612032	1.645 (0.136)	1.576 (0.186)	1.426 (0.223)	1.575 (0.292)	1.556 (0.214)	0.000998	5.42487
Steering Wheel Reversals [#]	38.679 (8.55)	34.25 (8.715)	22.679 (7.084)	26 (9.77)	25.286 (9.248)	7.52E-11	22.57442	24.929 (8.251)	23.071 (8.419)	20.75 (3.631)	21.786 (6.656)	20.464 (6.299)	0.263445	1.351727
Average driver torque [Nm]	0.169 (0.003)	0.096 (0.006)	0.147 (0.012)	0.105 (0.01)	0.101 (0.009)	5.32E-24	102.4083	0.165 (0.002)	0.045 (0.008)	0.056 (0.017)	0.046 (0.012)	0.044 (0.011)	1.81E-12	28.16731
						pValue	F(3,42)						pValue	F(3,42)
Time in conflict [%]		0.891 (0.719)	0.769 (0.719)	0.496 (0.386)	0.491 (0.374)	0.095478	2.270666		12.032 (10.869)	30.35 (14.137)	10.879 (10.06)	9.262 (5.561)	4.41E-06	13.16036
Average size of conflict [Nm]		0.041 (0.016)	0.048 (0.033)	0.034 (0.022)	0.029 (0.026)	0.285819	1.307088		0.041 (0.012)	0.06 (0.019)	0.047 (0.016)	0.041 (0.017)	0.000757	6.923615

TABLE VII
POST-HOC COMPARISONS AND SUBJECTIVE MEASURES ANOVA. A SIGNIFICANT DIFFERENCE IS INDICATED BY AN N FOR NARROW SECTIONS AND A W FOR WIDE SECTIONS. X WAS NOT MEASURED FOR SEPERATE ROAD CONDITIONS

			Pairwise Comparisons									
			M-L	M-H	M-S	M-A	L-H	L-S	L-A	H-S	H-A	S-A
Time out of bounds		Straights		N	N	N						
[%]		Curves			N			N				
Time to Lane Crossing		Straights	N	NW	N	N						
mean swath value [s]		Curves	W	W	N			N				
Time to Lane Crossing		Straights	W	NW	NW	NW						
mean minimum 10% [s]		Curves		W				N				
Steering Wheel Reversals		Straights		NW			NW			NW	NW	
[#]		Curves	NW	NW	NW	NW	N	N		N	N	
Average driver torque		Straights	N	NW	NW	NW	NW	N	N	W	W	
[Nm]		Curves		N	N	N	N	N	N			
Time in conflict		Straights					NW			NW	NW	
[%]		Curves					W				W	
Average size of conflict		Straights					N	N				
[Nm]		Curves					W			W	W	
RANOVA	pValue	F(3,56)	M-L	M-H	M-S	M-A	L-H	L-S	L-A	H-S	H-A	S-A
Workload	1.02E-05	9.241656	X	X	X	X						
Satisfaction	0.140599	1.811725										
Usefulness	0.013881	3.465857		X	X							

A

Motivation of the independent variable selection in adaptive LoHA

The choice for Time to Lane Crossing (TLC) as the independent variable in adaptive LoHA was made after a comparison of several metrics found in literature. Candidate parameters were mainly taken from my own previous literature research on adaptive systems, Scholten's (2017) [10] literature review on conflicts in driving with haptic shared control, the literature review of Cain(2007) [3] on the measurement of operator workload and a literature review by Johansson(2004)[4] on metrics for the assessment of ADAS systems. The following inclusion criterions were applied for the candidate metrics:

- The metrics have to be objective.
- The metrics have to be quantifiable.
- It has to be feasible to determine the metrics during a driving task in the HMI-lab at the faculty of aerospace engineering.

The collected metrics are grouped per theme in Table A.1.

Table A.1: Considered metrics for an adaptive LoHA system, categorised by category.

Scenario	**Performance**	**Conflict**	**Workload**
Roadwidth [13]	Time to lane crossing [4]	Magnitude of conflict [8]	Heart rate (variability) [3]
Velocity [4]	Steering movements [4]	Neuromuscular admittance [11]	Blink rate [3]
Bandwidth [9]	Heading error [4]	Trajectory deviation [8]	Secondary task performance [3]
Traffic density	Lateral error [4]		Elektro-encefalografie (EEG) [3]
			Galvanic Skin Resistance (transpiration) [3]

The fitness of a metric is based upon the type of data it provides, the objectivity and which factors of HSC affect it (Environment, Driver, and Controller). Out of the fittest metrics, Time to Lane crossing was chosen because in addition to fulfilling all requirements, it incorporated effects of three other candidates in addition to a predictive element.

Table A.2: Scoring system for judging a metric's fitness

	Data-type	Objective	Environment related	Operator related	Controller related	Score
Roadwidth	Ratio	Yes	Yes	No	No	3
Velocity	Ratio	No	Yes	Yes	No	3
Bandwidth	Interval/Ratio	Yes	Yes	Yes	Yes	3.5
Obstacles/traffic	Interval	Yes	Yes	No	No	2.5
TLC/TTC	Ratio	Yes	Yes	Yes	Yes	**5**
Heading error	Ratio	Yes	Yes	Yes	Yes	**5**
Lateral error	Ratio	Yes	Yes	Yes	Yes	**5**
Torque conflicts	Ratio	Yes	No	Yes	Yes	4
NMS admittance	Ratio	Partial	No	Yes	No	2.5
Trajectory variability	Ratio	Yes	Yes	Yes	Yes	**5**
Heart rate	Ratio	Yes	No	Yes	No	3
Blink rate	Ratio	Partial	Partial	Yes	No	3
Skin resistance	Ratio	Yes	No	Yes	No	3
Secondary task	Interval/Ratio	Yes	Partial	Yes	No	3

B

Design of a Haptic Steering Wheel

This appendix describes the steps in designing a haptic steering wheel that provides active steering assistance and stiffness feedback.

B.1. Dynamic Steering Wheel Model

The implementation of a haptic steering wheel begins with the description of a plain steering wheel. The steering wheel and column of a car can be modelled as a mass-spring-damper system (B.1).

$$\tau = I_{sw}\ddot{\omega} + B_{sw}\dot{\omega} + K_{sw}\omega \tag{B.1}$$

Where the Inertia I_{sw} and Damping B_{sw} are passive properties of the system while the stiffness K_{sw} is a simplified stiffness representing the linearised result of the car's self-aligning torque due to the cornering force and pneumatic trail. By restructuring the equation to (B.2) we arrive at a form that can be drawn as a flowchart B.1.

$$\ddot{\omega} = \frac{1}{I_{sw}}(\tau - B_{sw}\dot{\omega} - K_{sw}\omega) \tag{B.2}$$

This describes the dynamic behaviour of a loose steering wheel but during driving it is held by the driver who will add his own dynamic properties to the system, for small movements the human muscle can also be described a mass-spring-damper system [12]. The inertia I_{nms} is a passive property of the human arm while damping B_{nms} and stiffness K_{nms} have an active component that the driver can adjust in addition to their passive properties . The active damping component is not taken into account in this model since it is relatively small compared to the passive damping , furthermore the additional stiffness and damping resulting from reflexive feedback are described as a part of the passive arm properties.

Contrary to the car's self-aligning torque, the human stiffness can work around any desired steering wheel position which will be denoted as ω_{hu} [12]. The human dynamic system is described by equation (B.3). Combining and restructuring (B.1) and (B.3) yields the total steering wheel interaction (B.4).

$$\tau = I_{hu}\ddot{\omega} + B_{hu}\dot{\omega} + K_{hu}(t)(\omega_{hu} - \omega) \tag{B.3}$$

$$\tau = (I_{sw} + I_{hu})\ddot{\omega} + (B_{sw} + B_{hu})\dot{\omega} + K_{sw}\omega + K_{hu}(t)(\omega_{hu} - \omega) \tag{B.4}$$

Since we are not just modeling a passive steering wheel but a haptic one that gives stiffness feedback around the controller's desired steering wheel position denoted as ω_{au} we will add one more active component to the steering wheel that mirrors the human dynamics and then group the terms according to the input signals B.6.

$$\tau = (I_{sw} + I_{hu})\ddot{\omega} + (B_{sw} + B_{hu})\dot{\omega} + K_{sw}\omega + K_{hu}(t)(\omega - \omega_{hu}) + K_{au}(t)(\omega - \omega_{au}) \tag{B.5}$$

$$\tau = (I_{sw} + I_{hu})\ddot{\omega} + (B_{sw} + B_{hu})\dot{\omega} + (K_{sw} + K_{hu} + K_{au})\omega - K_{hu}(t)\omega_{hu} - K_{au}(t)\omega_{au} \tag{B.6}$$

The total system dynamics are visualized in a flowchart B.2.

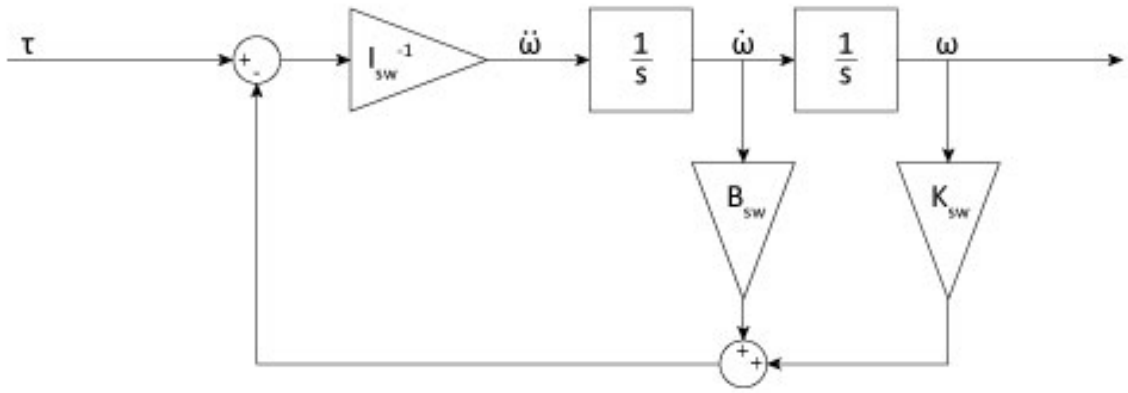

Figure B.1: Flowchart of the steering wheel dynamics

B.2. Torque Generation

The assisting controller that provides guidance to the driver calculates the desired steering wheel angles to follow a trajectory but these need to be translated to torques before they can be fed to the haptic steering wheel. Because we just modelled the steering wheel dynamics, the inverse of this model can be used to create the perfect feed-forward signal [1]. Human operators are known to create an internal model of dynamic systems for feed forward control [5] so for simulation they can be modelled as a mirror image of the feed forward controller.

While theoretically sound this method has a limitation in real world implementation: although it is reasonable to assume both agents have good estimates of the steering wheel's passive properties as well as their own. Neither agent knows nor can properly estimate the dynamic properties and desired steering wheel angle of each other. Also, we do not want the feed forward signal of both agents to attempt to cancel each other out or we will enter a loop where both controllers are ramping up their torques to cancel out the other's also increasing torques. This is why the human dynamics will not be included in the controller's internal model and vice versa. First the system's transfer function (B.7) is obtained from the Laplace transform (B.8) of the steering wheel dynamics.

$$H(s) = \frac{Y(s)}{X(s)} \tag{B.7}$$

$$F(s) = \int_0^\infty f(t)e^{-st}dt \tag{B.8}$$

The system is considered a MISO system (multiple inputs, single output) where three inputs, the incoming torque (τ) and the agents' desired angles ($\omega_{hu} - \omega$) and ($\omega_{au} - \omega$), result in a steering wheel angle (ω). This particular MISO system can be decomposed in a sum three SISO systems.

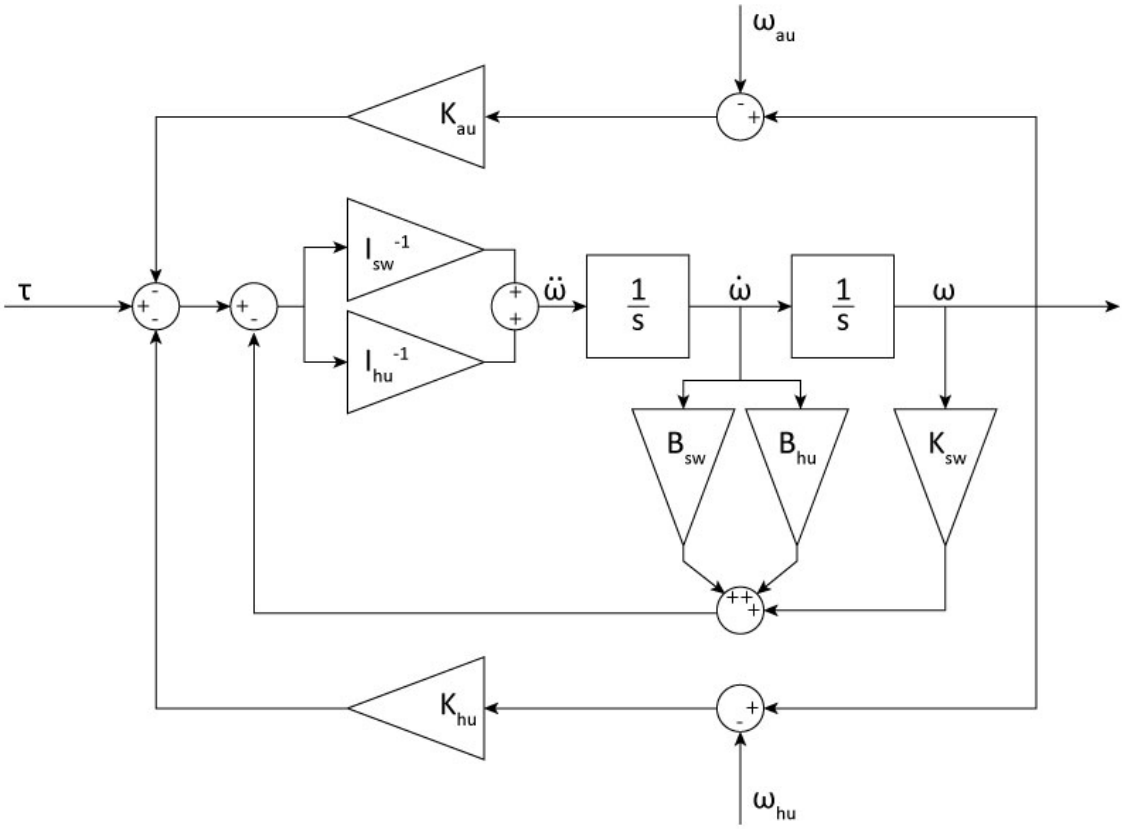

Figure B.2: Flowchart of the total interaction dynamics

$$\omega(s) = H_1\tau(s) + H_2\omega_{hu}(s) + H_3\omega_{au}(s) \tag{B.9}$$

$$H_1(s) = \frac{1}{(I_{sw}+I_{hu})s^2 + (B_{sw}+B_{hu})s + (K_{sw}+K_{hu}+K_{au})} \tag{B.10}$$

$$H_2(s) = \frac{K_{hu}}{(I_{sw}+I_{hu})s^2 + (B_{sw}+B_{hu})s + (K_{sw}+K_{hu}+K_{au})} \tag{B.11}$$

$$H_3(s) = \frac{K_{au}}{(I_{sw}+I_{hu})s^2 + (B_{sw}+B_{hu})s + (K_{sw}+K_{hu}+K_{au})} \tag{B.12}$$

Now the transfer function (B.9) can be inverted to calculate (τ). Since we want ω to equal the desired steering wheel angle it will be substituted in the solution.

$$\tau(s) = H_1^{-1}\omega(s) - H_1^{-1}H_2\omega_{hu}(s) - H_1^{-1}H_3\omega_{au}(s) \tag{B.13}$$

$$H_1^{-1} = (I_{sw}+I_{hu})s^2 + (B_{sw}+B_{hu})s + (K_{sw}+K_{hu}+K_{au}) \tag{B.14}$$

$$H_1^{-1}H_2 = K_{hu} \tag{B.15}$$

$$H_1^{-1}H_3 = K_{au} \tag{B.16}$$

However, the inverse transfer function (B.14) is improper: the order of the numerator exceeds the order of the denominator, and thus is non-causal. To make the system causal again, a second order Butterworth filter [2] is added (B.17) to filter out the high frequency responses. This is not a problem since the natural human response has a cut-off frequency (ω_c) of three Hertz, this will also be the cut-off frequency of the Butterworth filter. The controller's cut-off frequency is system dependent and can be separately designed but will be set

to mirror the human driver in this derivation.

$$H_1^{-1} \rightarrow \frac{(I_{sw}+I_{hu})s^2+(B_{sw}+B_{hu})s+(K_{sw}+K_{hu}+K_{au})}{(\frac{s}{\omega_c})^2-(\lambda_1+\lambda_2)\frac{s}{\omega_c}+\lambda_1\lambda_2} \tag{B.17}$$

$$\lambda_{k(1,2)} = e^{\frac{i\pi}{2n}(2k-1+n)} \tag{B.18}$$

By ruling out the unknown dynamics of the other agent we are left with the two feed forward controllers.

$$\tau_{hu}(s) = \frac{(I_{sw}+I_{hu})s^2+(B_{sw}+B_{hu})s+(K_{sw}+K_{hu})}{(\frac{s}{\omega_c})^2-(\lambda_1+\lambda_2)\frac{s}{\omega_c}+\lambda_1\lambda_2}\cdot\omega(s) - \frac{K_{hu}\omega_{hu}(s)}{(\frac{s}{\omega_c})^2-(\lambda_1+\lambda_2)\frac{s}{\omega_c}+\lambda_1\lambda_2} \tag{B.19}$$

$$\tau_{au}(s) = \frac{I_{sw}s^2+B_{sw}s+(K_{sw}+K_{au})}{(\frac{s}{\omega_c})^2-(\lambda_1+\lambda_2)\frac{s}{\omega_c}+\lambda_1\lambda_2}\cdot\omega(s) - \frac{K_{au}\omega_{au}(s)}{(\frac{s}{\omega_c})^2-(\lambda_1+\lambda_2)\frac{s}{\omega_c}+\lambda_1\lambda_2} \tag{B.20}$$

Since the controllers aim for $\omega(t)$ to equal their own internal $\omega_{hu}(t)$ and $\omega_{au}(t)$, the equations for feedforward control are further reduced to:

$$\tau_{hu}(s) = \frac{(I_{sw}+I_{hu})s^2+(B_{sw}+B_{hu})s+K_{sw}}{(\frac{s}{\omega_c})^2-(\lambda_1+\lambda_2)\frac{s}{\omega_c}+\lambda_1\lambda_2}\cdot\omega_{hu}(s) \tag{B.21}$$

$$\tau_{au}(s) = \frac{I_{sw}s^2+B_{sw}s+K_{sw}}{(\frac{s}{\omega_c})^2-(\lambda_1+\lambda_2)\frac{s}{\omega_c}+\lambda_1\lambda_2}\cdot\omega_{au}(s) \tag{B.22}$$

B.3. Human Simulation

The previous section discussed the ideal torque generation of the simulation as it would be in an ideal system, the human body however is not ideal but works with time delays and activation dynamics. To create a more accurate simulation of human behaviour these factors have to be implemented in the model

First of all the Human Central Nervous System has a processing delay , according to McRuer this delay differs from person to person between 0.1 and 0.2 seconds [6]. In the model this is implemented by a pure signal delay that is placed before the feed forward controller.

$$G_\tau(s) = e^{-s\tau} \tag{B.23}$$

Furthermore the human skeletal muscle has an activation lag that can be approximated by a first order low pass filter [**?**]. This filter is placed after torque generation to filter the output.

$$G_{nms}(s) = \frac{1}{T_N s+1} \tag{B.24}$$

Lastly the human system has some inherent motor noise that is muscle and individual dependent as well as directly proportional to the muscle activation. In this simulation the human motor noise will be represented by a scaling white noise on the human torque that has a standard deviation equal to 2% of the output torque.

B.4. Position Feedback

Up till now we have only looked at the orientation of the steering wheel but the objective in driving is not to achieve a certain steering wheel angle but to follow a trajectory and stay on the road. The actual car trajectory that is followed is an integration of the steering wheel output over time.

The feed forward controller that has now been implemented only accounts for the heading angle but not for any positional errors. As such we do not only need a controller that follows the optimal heading angle but also a corrective feedback controller that steers the car towards a desired trajectory and eliminates offsets.

The solution for this problem is implemented by [14] where the feedback torque is decoupled from the feedforward controller and calculated by a separate weighting factor called the Strength of Haptic Feedback (SoHF).

$$\tau_{FB} = K_{SoHF} \cdot \Delta\psi \tag{B.25}$$

B.5. Clustering the force generating components

In the previous sections we have gradually constructed all components of agent - steering wheel interaction but the forces that are generated by each agent are currently distributed over several components: the feed-forward controller, the steering wheel interaction dynamics and the feedback controller. By grouping these components as in figure B.3 we get insights in the total force generation of each agent and the steering wheel response.

Because there are two controllers that aim to follow trajectory the inputs are twice the actual amount that is needed to steer the car. To correct for this we introduce a weighted scaling factor called the 'Level of Haptic Support' (LoHS) [7]. This factor is a measure of how much of the required steering input is supplied by the controller, the remaining input is to be supplied by the driver. At a LoHS of 1 the car is fully automated while at 0 the car is manually driven. With this variable we can design the controller do supply different levels of support.

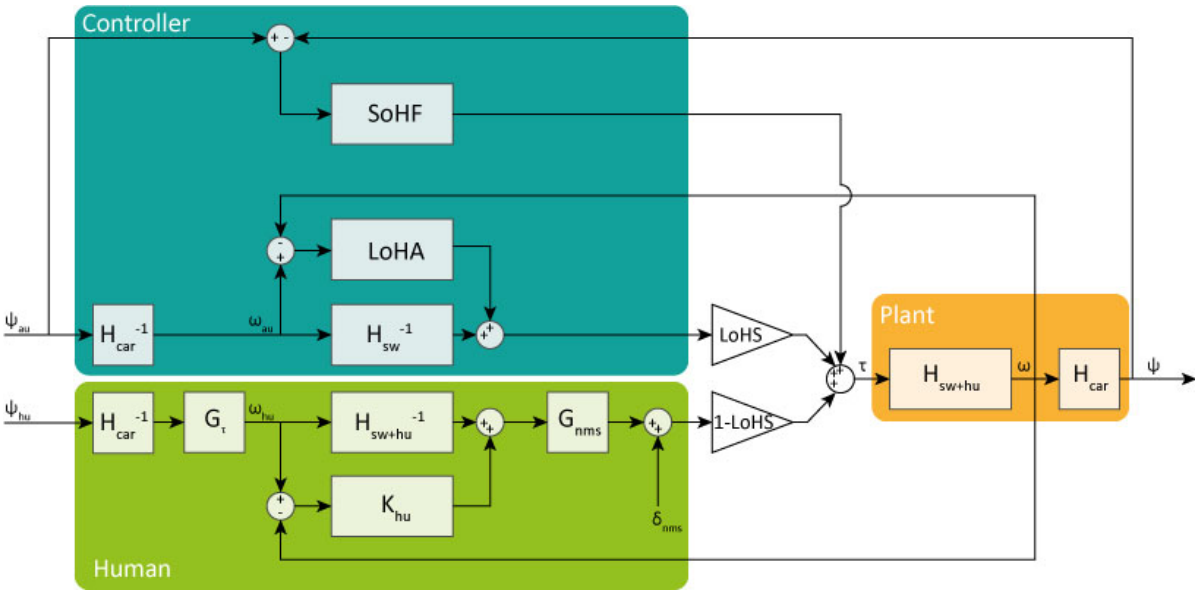

Figure B.3: Flowchart of the total plant control loop

B.6. Model Simulation

Given this model there are three parameters that the system designer can freely tune to influence the response of the car and the driver: the LoHA, LoHS and SoHF, furthermore the driver can adjust his own stiffness K_{hu}. In this section we will discuss the effects of each parameter on the plant performance and the human force profile.

Unless specified otherwise, the simulations were performed with the parameters of table B.1. The human dynamics can vary greatly but the values where chosen within the range of a relax task.

Simulation 1

First we will observe the steering wheel angles and agent torques while driving a sinusoidal trajectory without feedback controller. A disturbance with a $STD = 0.1 rad$ at $1 Hz$ is applied to the output steering wheel angle. It can be observed in figure B.4 that the tracking is good and the generated torques are not influenced by the LoHA. This is to be expected since LoHA only affects the error between the feedforward signal and the actual steering wheel angle which is very small in this instance. Note that when the LoHA equals 0, there is no influence of the steering wheel disturbance on the controller torque because of the lack of a feedback gain. As LoHA increases the controller's response to disturbances is observed to also increase as expected.

Table B.1: Model Parameters

Parameter	Value	
K_{hu}	5.0	$\left[\frac{Nm}{rad}\right]$
B_{hu}	0.2	$\left[\frac{Nms}{rad}\right]$
I_{hu}	0.3	$\left[\frac{Nms^2}{rad}\right]$
K_{sw}	4.2	$\left[\frac{Nm}{rad}\right]$
B_{sw}	2.0	$\left[\frac{Nms}{rad}\right]$
I_{sw}	0.3	$\left[\frac{Nms^2}{rad}\right]$
K_{au}	5.0	$\left[\frac{Nm}{rad}\right]$
τ_{nms}	0.1	$[s]$
T_N	0.1	–

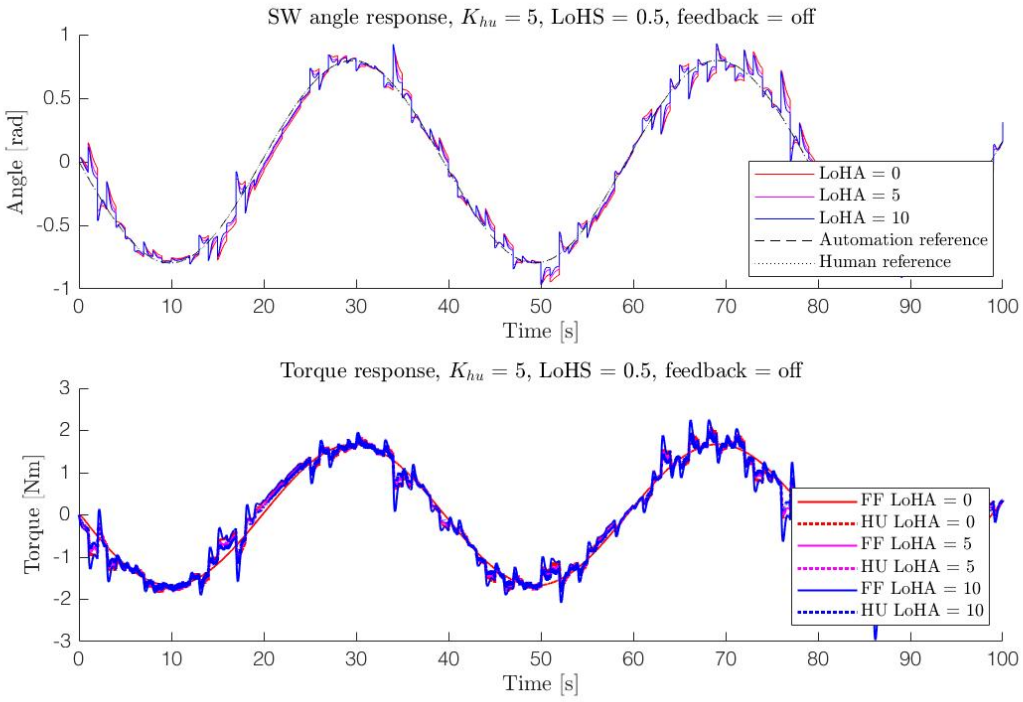

Figure B.4: SW angle and torque for sine tracking under different LoHAs

Simulation 2

While the system was designed to have a combined total steering contribution of 100%, in reality this might not be the case. To investigate this scenario Figure B.5 shows the response to a 'mismatched' total feed forward command that is only half, full or double the required amount, split evenly between the driver and controller. The full command scenario is the same as previously displayed in figure B.4

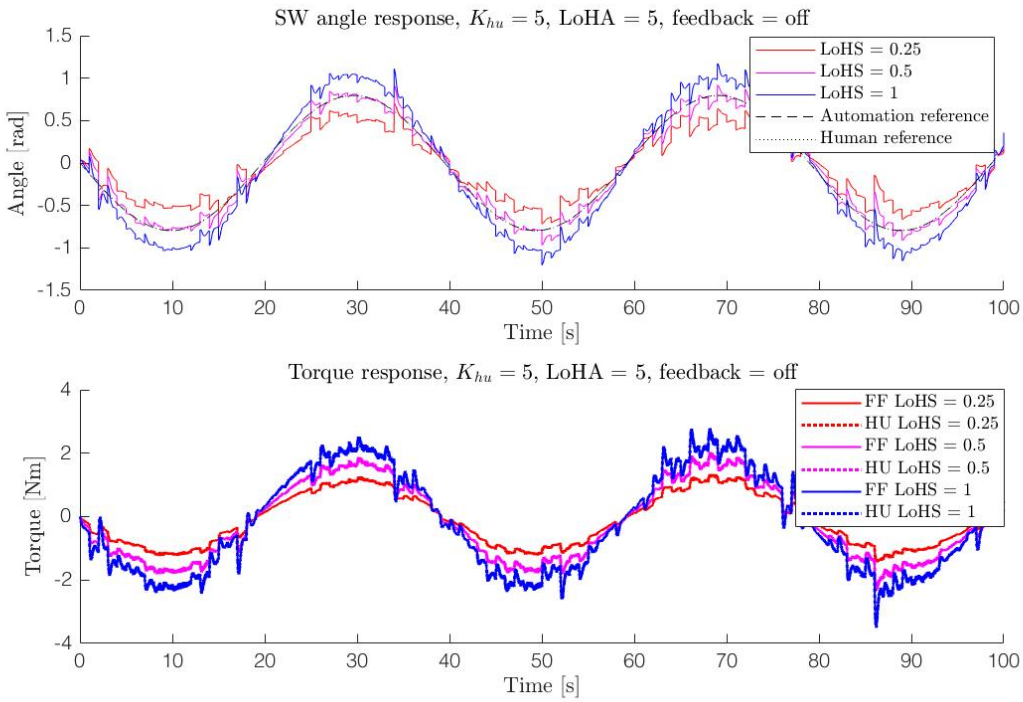

Figure B.5: SW angle and torque for sine tracking under different LoHSes

Although the mismatched feed forward commands are half or double the required amount, the steering wheel response and agent torques are much closer to the required value. This is because of the feedback through $LoHA$ and K_{hu}, as these increase compared to K_{sw} the effect of a mismatch in the LoHS will decrease.

Although the mismatched feed forward commands are half or double the required amount, the steering wheel response and agent torques are much closer to the required value. This is because of the feedback through $LoHA$ and K_{hu}, as these increase compared to K_{sw} the effect of a mismatch in the LoHS will decrease.

Simulation 3

Because the feed forward model of the controller does not include the Human damping and inertia, there is a mismatch in the feed forward dynamics when the human holds steering wheel. These effects become apparent at higher frequency tracking signals which is why we will look at a step response with and without the driver passively holding the steering wheel in figure B.6. Table B.2 contains a brief recap of which agent contains which dynamics in its feed forward controller.

Table B.2: Simulation settings

agent	dynamics	matching
controller	sw	match
controller	sw+hu	mismatch
driver	sw+hu	match

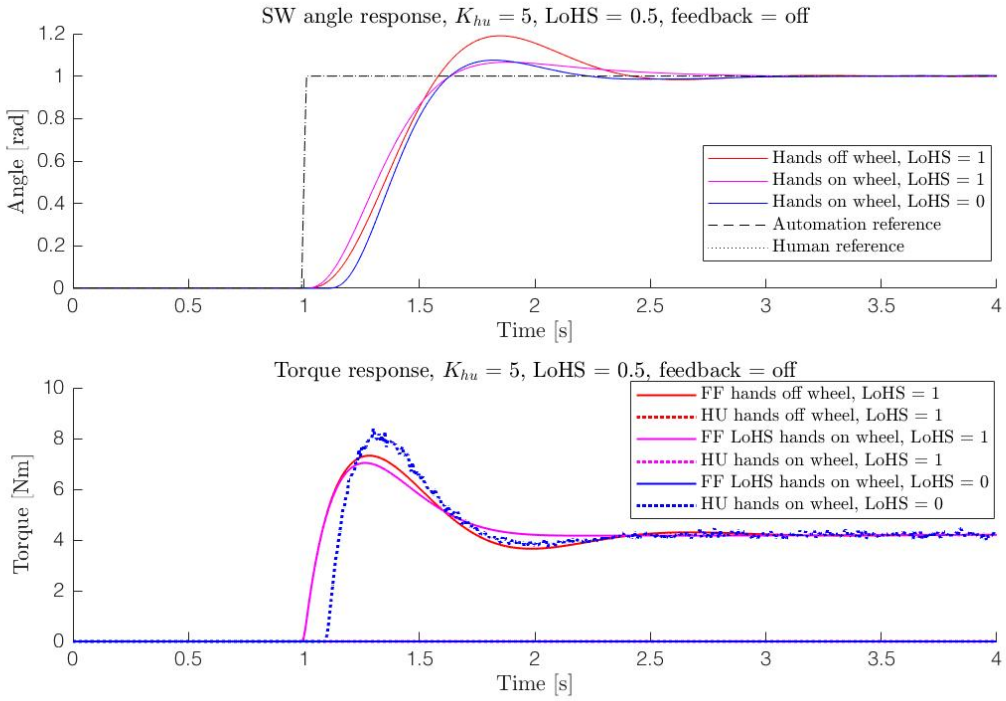

Figure B.6: SW angle and torque for sine tracking under different LoHAs

First of all we can see that all systems in the current settings (Table:B.1) are under-damped which which explains why the 'mismatched' feedforward controller performs better than the matched controllers: the extra damping and inertia bring the system closer to a critical damping and thus a faster step-response.
Still the error is rather small which might be explained by the human damping coefficient being very small ($\frac{1}{10}^{th}$) relative to that of the steering wheel (see table: B.1).

$$\zeta = \frac{B}{2\sqrt[2]{I \cdot K}} \tag{B.26}$$

Since the steering wheel damping and inertia are design parameter we might want to use them and to bring the system close to critical damping (B.26) and use the LoHA; the big influencing factor in the damping ratio that the automation controls, to adjust the damping ratio for human fluctuations. and as such the damping criticality may be an interesting factor in its tuning.

Simulation 4
Up till now we have looked at the steering wheel response under agreement of the operators. In reality there will almost always be a difference between the trajectories each agent tries to follow. In this simulation (Figure B.7) we observe how LoHA and LoHS affect the balance between the agents with a 180 degree phase difference or opposed steering command.

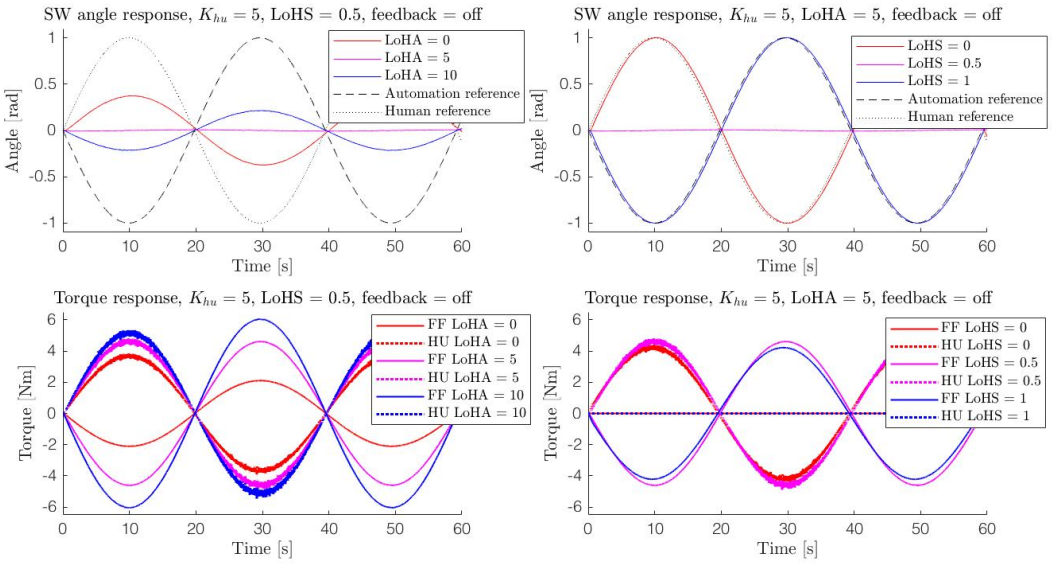

Figure B.7: SW angle and torque for sine tracking under different LoHAs, LoHSes and inputs

On the left hand side we observe the effect of the controller stiffness or LoHA, at equal stiffness with the human operator the feed forward commands will exactly cancel out while higher or lower a relative stiffness will push the steering wheel response towards the controller and human trajectory respectively. Note two things: the LoHA in itself cannot fully reject the human as it only responds to trajectory *deviations*, LoHA only approaches the desired trajectory in the limit. Furthermore, as the LoHA increases so does the human torque response due to the increased deviation from his own desired trajectory.

On the right side we observe a similar graph for the input division LoHS. A changing LoHS presents a smooth trajectory transition dependent on the input fractioning. Contrary to transitioning with the LoHA, the torques move between 0% to a peak value and back to 100%. Do note that while the total input command is 100% in this simulation, the algorithm will in reality only control the automation's steering input fraction while the driver simply increases his fraction to reach the desired state

Simulation 5

Not only the LoHA can change but the human driver can adjust his K_{hu} in similar fashion, a comparison between these parameters is displayed in figure B.8 where both controllers respond to a delayed step input. The reference trajectories as such as matched(0-1s)-mismatched(1-4s)-matched(4-7s). Again we see that increasing one agents stiffness shifts the steering wheel response towards that agent's desired trajectory while also increasing both input torques. We can also observe that after an initial transient response the steady state of both controllers is exactly mirrored at equal stiffnesses.

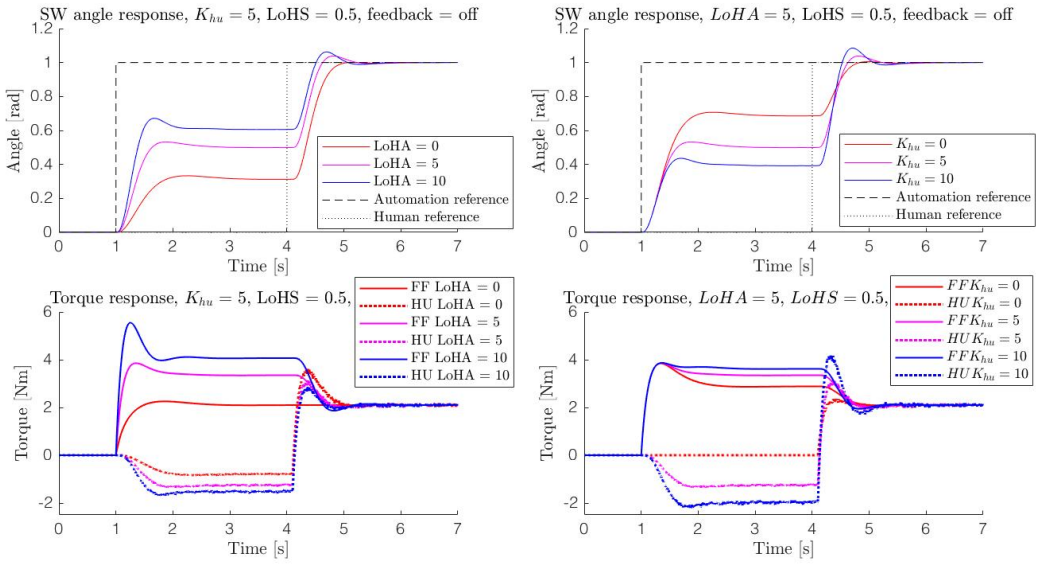

Figure B.8: SW angle and torque for sine tracking under different LoHAs

Simulation 6

Up till now we have only looked at the steering wheel responses but not at that of the car (represented by an integrator in this simulation). To observe the effect of the positional feedback controller gain (SoHF) which corrects integration offsets we do not only have to look at the steering wheel motion but also the heading error of the vehicle. In the following plots (Figure B.9 & B.10) the car is set to drive in a straight line but the car has an orientation error of one radian. The feed forward controller wants to keep the car straight, while the feedback controller wants to correct the heading error.

Here we see the clear benefit of the additional feedback controller, since any constant offset is lost when the car's state is differentiated, the feed forward controller does not correct the vehicle heading. The additional SoHF solves this problem. Do note that the feedback response does invoke an opposite response of the feed forward controllers since it wants to turn the steering wheel while they want to drive straight. The final steering wheel response is at the equilibrium between the LoHA + K_{hu} and the SoHF. The counteraction of LoHA and LoHS should be carefully considered when adjusting either.

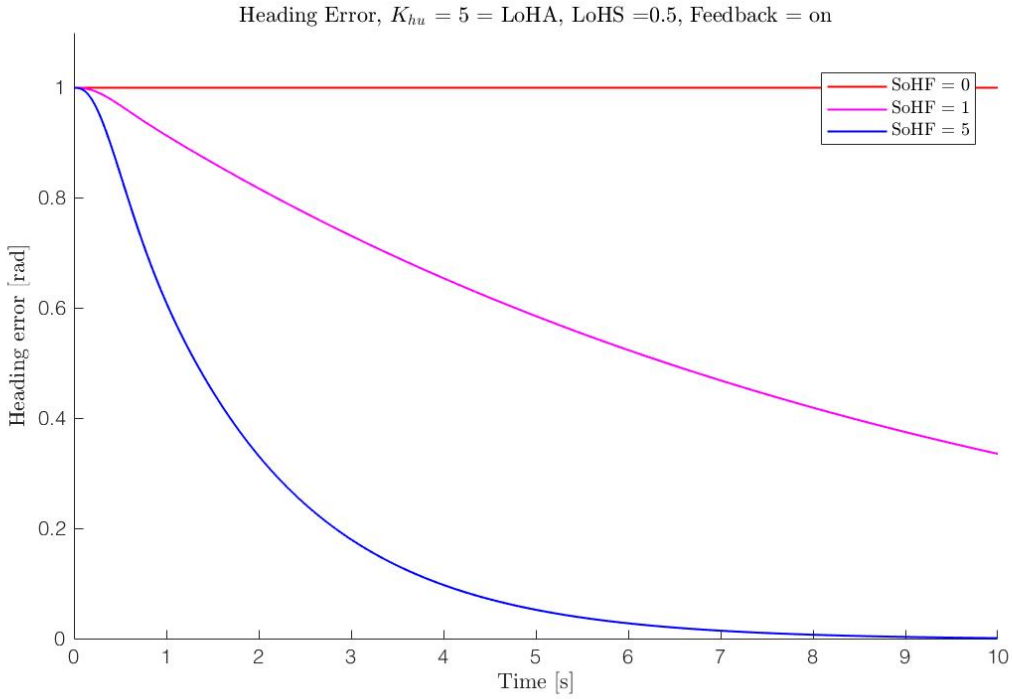

Figure B.9: Heading error after an initial offset of 1 radian for different LoHS gains

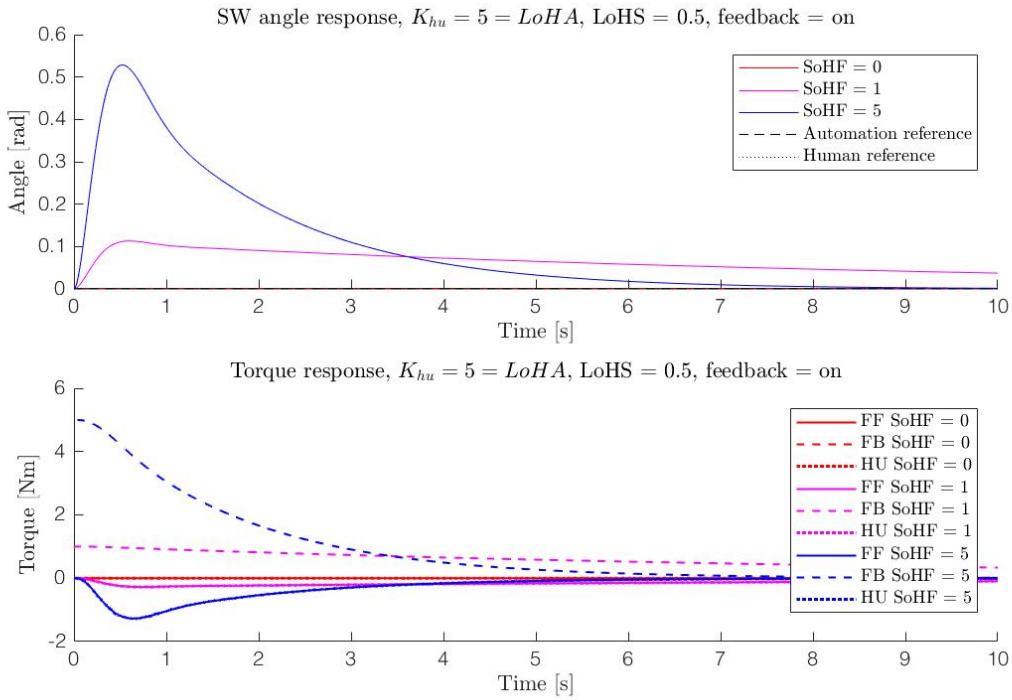

Figure B.10: SW angle and torque response for an initial heading offset for different SoHF gains

Bibliography

[1] David A. Abbink, Mark Mulder, and Erwin R. Boer. Haptic shared control: Smoothly shifting control authority? *Cognition, Technology and Work*, 14(1):19–28, 2012. doi: 10.1007/s10111-011-0192-5.

[2] Stephen Butterworth. On the theory of filter amplifiers, 1930.

[3] Brad Cain. A Review of the Mental Workload Literature. *Defence research and development Toronto (Canada)*, (1998):4–1–4–34, 2007. URL http://www.dtic.mil/cgi-bin/GetTRDoc?Location=U2{&}doc=GetTRDoc.pdf{&}AD=ADA474193.

[4] E Johansson, J Engström, C Cherri, E Nodari, A Toffetti, R Schindhelm, and C Gelau. Review of existing techniques and metrics for IVIS and ADAS assessment. *Aide Project*, (March):1–93, 2004.

[5] Mitsuo Kawato. Internal Models for Motor Control and Trajectory Planning., 1999. ISSN 09594388. URL http://dx.doi.org/10.1016/S0959-4388(99)00028-8.

[6] D. McRuer. Human Dynamics in Man-Machine Systems. 16, 1980.

[7] M. M. Van Paassen, R. Boink, D. A. Abbink, Mark. Mulder, and Max. Mulder. Four design choices in Haptic shared control. In *Advances in Aviation Psychology, Volume 2: Using Scientific Methods to Address Practical Human Factors Needs*, chapter 12, pages 237 – 254. 2017. ISBN 131718520X. URL https://books.google.nl/books?hl=nl{&}lr={&}id=8iolDwAAQBAJ{&}oi=fnd{&}pg=PA237{&}dq=Four+design+choices+for+haptic+shared+control,{&}ots=3dIY4HZOEx{&}sig=xSM77hpZWJkiQy2c5BfBX2WEBGY{#}v=onepage{&}q=Fourdesignchoicesforhapticsharedcontrol{%}2C{&}f=false.

[8] Carolina Passenberg, Antonia Glaser, and Angelika Peer. Exploring the design space of haptic assistants: The assistance policy module. *IEEE Transactions on Haptics*, 6(4):440–452, 2013. ISSN 19391412. doi: 10.1109/TOH.2013.34.

[9] Sebastiaan M. Petermeijer, David A. Abbink, and Joost C.F. de Winter. Should Drivers Be Operating Within an Automation-Free Bandwidth? Evaluating Haptic Steering Support Systems With Different Levels of Authority. *Human Factors: The Journal of the Human Factors and Ergonomics Society*, 57:5–20, 2014. ISSN 0018-7208. doi: 10.1177/0018720814563602. URL http://hfs.sagepub.com/content/57/1/5.hort.

[10] Wietske M Scholtens. Methods to reduce conflicts in Haptic Shared Control (MSc literature review). Technical report, 2017.

[11] Jan Smisek, Student Member, Emmanuel Sunil, Marinus M Van Paassen, Senior Member, David A. Abbink, and Mark Mulder. Neuromuscular-System-Based Tuning of a Haptic Shared Control Interface for UAV Teleoperation. pages 1–13, 2016.

[12] Frans C T Van Der Helm, Alfred C. Schouten, Erwin De Vlugt, and Guido G. Brouwn. Identification of intrinsic and reflexive components of human arm dynamics during postural control. *Journal of Neuroscience Methods*, 119(1):1–14, 2002. ISSN 01650270. doi: 10.1016/S0165-0270(02)00147-4.

[13] Daan W J Van Der Wiel, Marinus M. Van Paassen, Mark Mulder, and David A. Abbink. Driver Adaptation to Driving Speed and Road Width: Exploring Parameters for Designing Adaptive Haptic Shared Control. *Proceedings - 2015 IEEE International Conference on Systems, Man, and Cybernetics, SMC 2015*, pages 3060–3065, 2015. doi: 10.1109/SMC.2015.532.

[14] P Wyzen, Marinus M. Van Paassen, and D. A. Abbink. Separating Haptic Guidance and Support Signals : a Solution for Human-Machine Cooperation ? (MSc thesis). Technical report, 2017.

C

Supplementary data plots

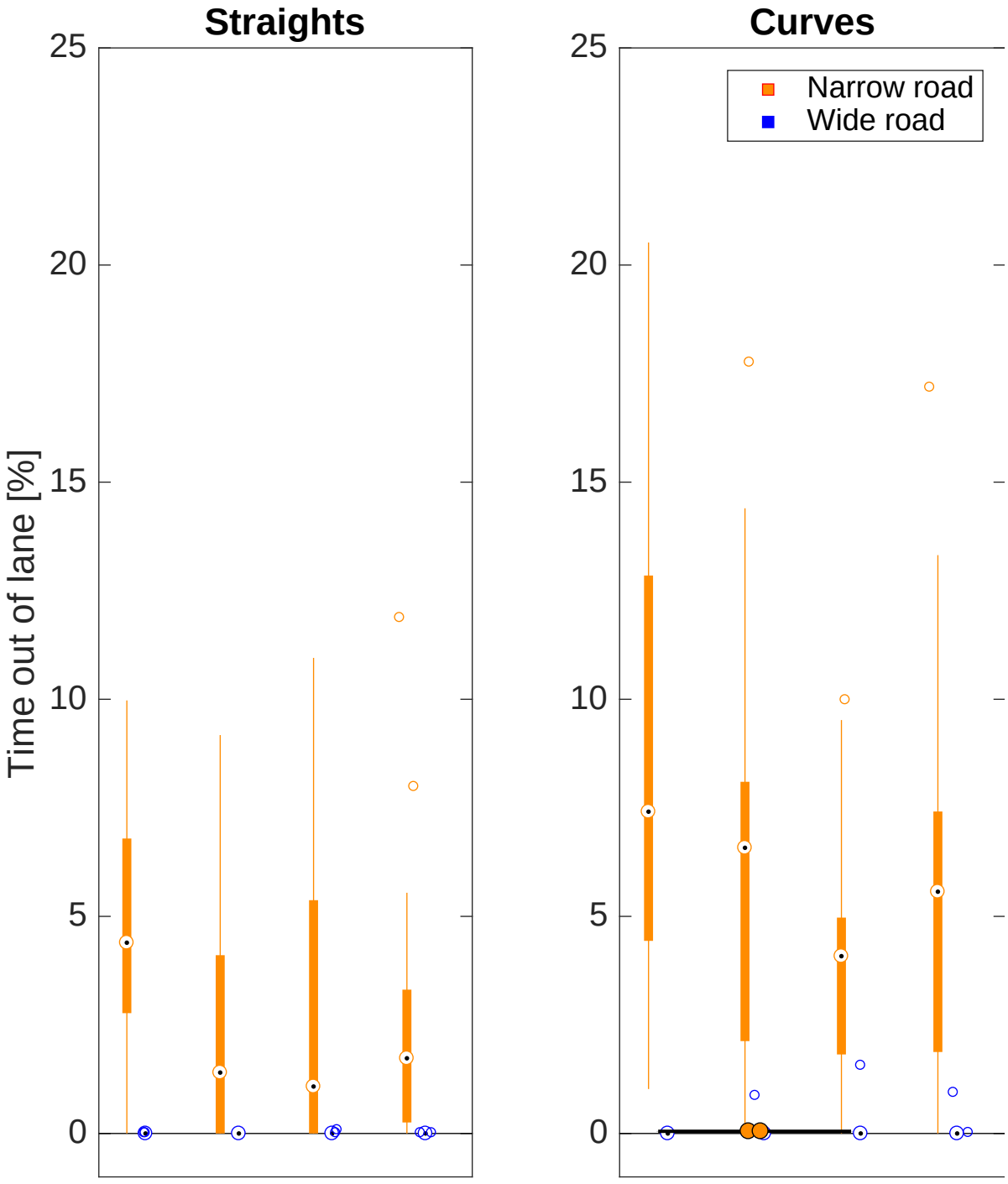

Figure C.1: Time out of lane.

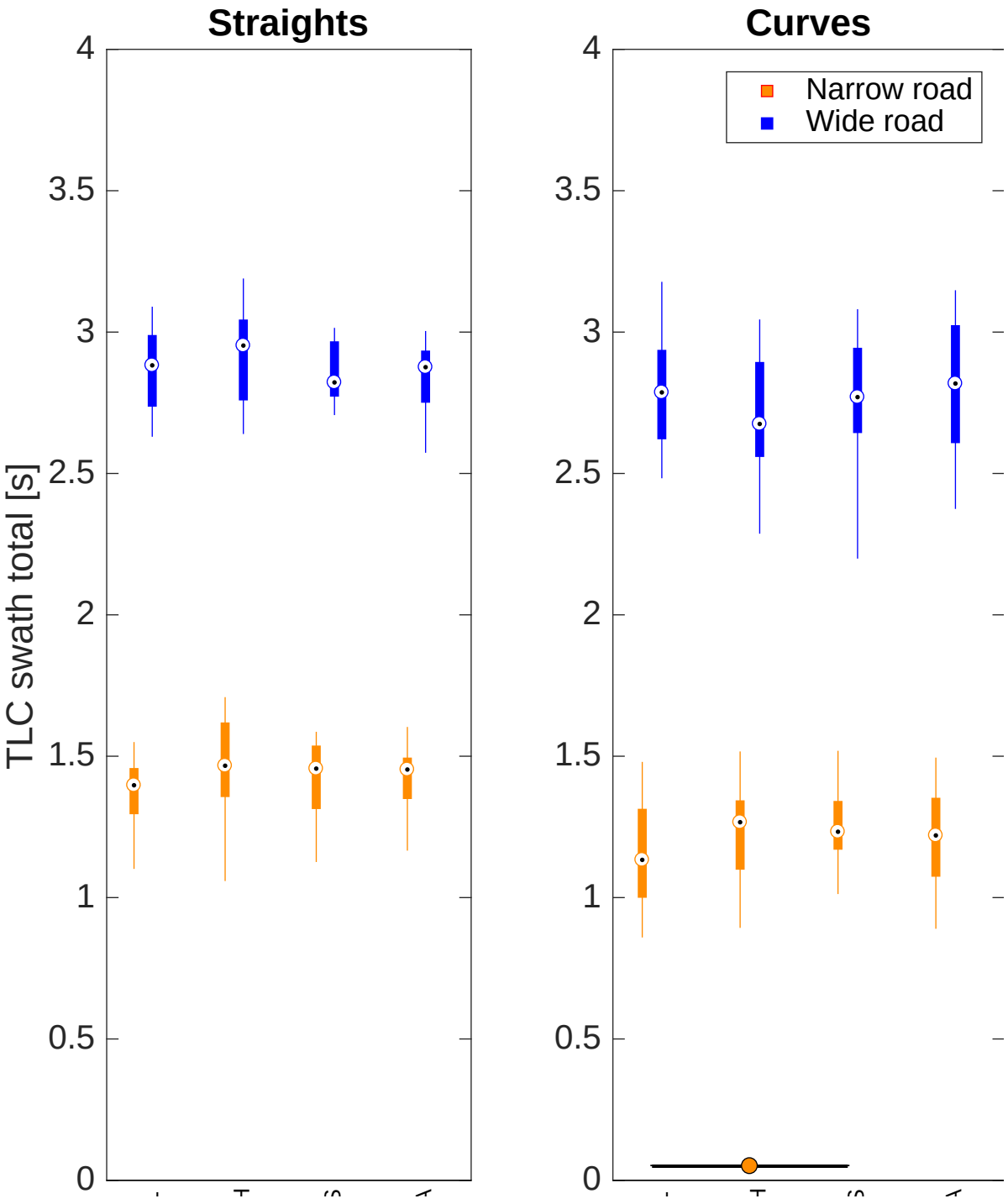

Figure C.2: TLC.

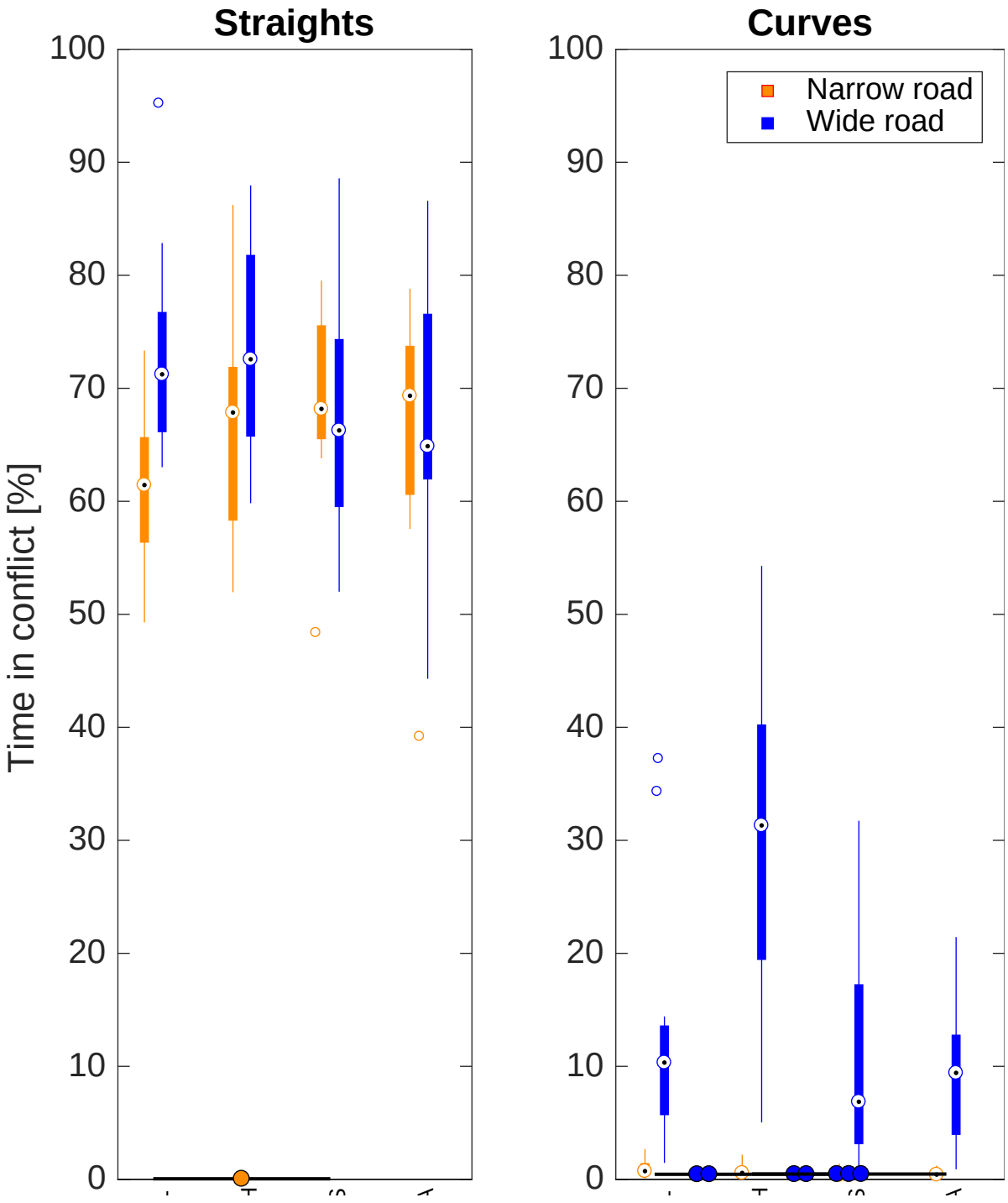

Figure C.3: Time spent in conflict.

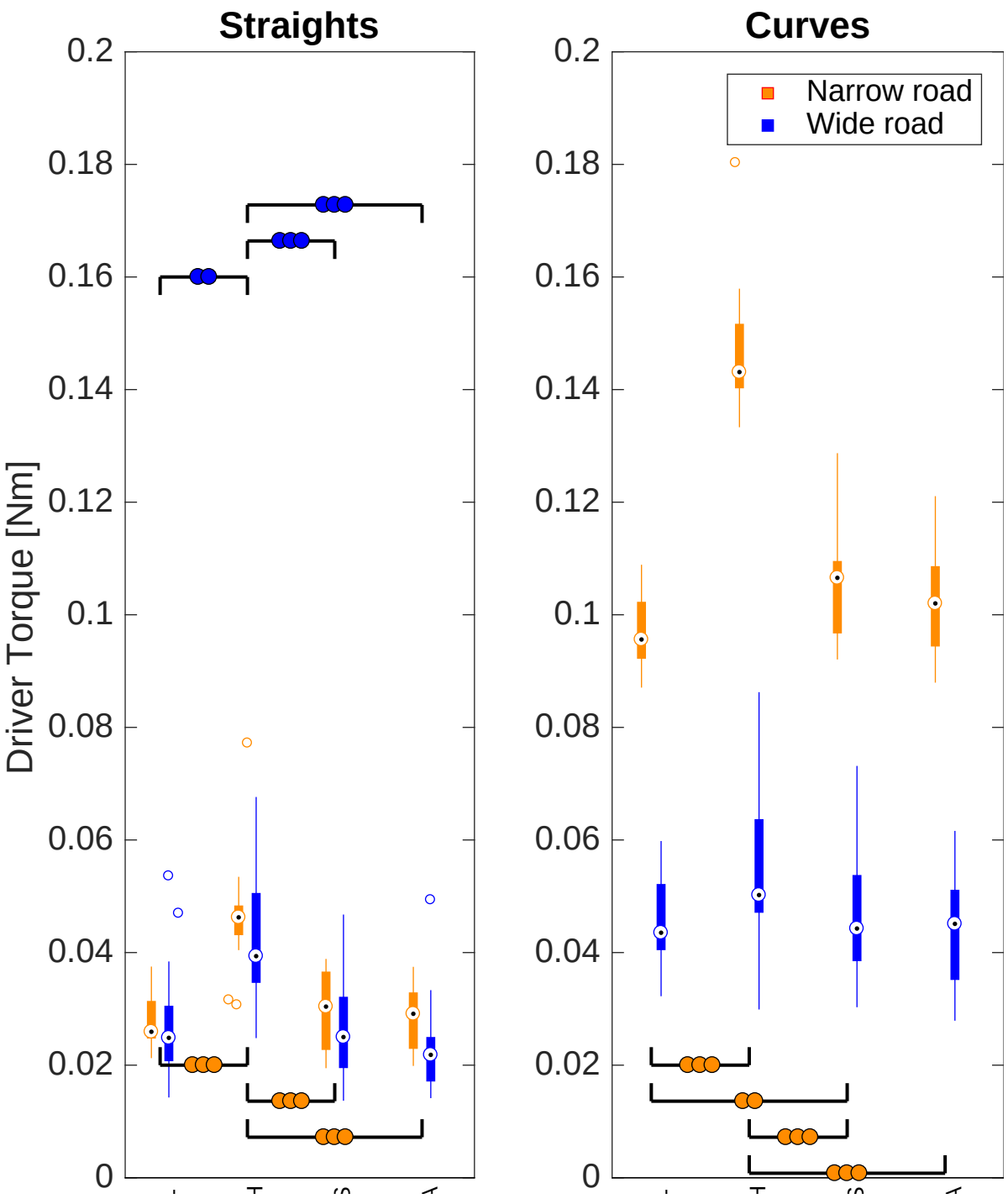

Figure C.4: Driver torques.

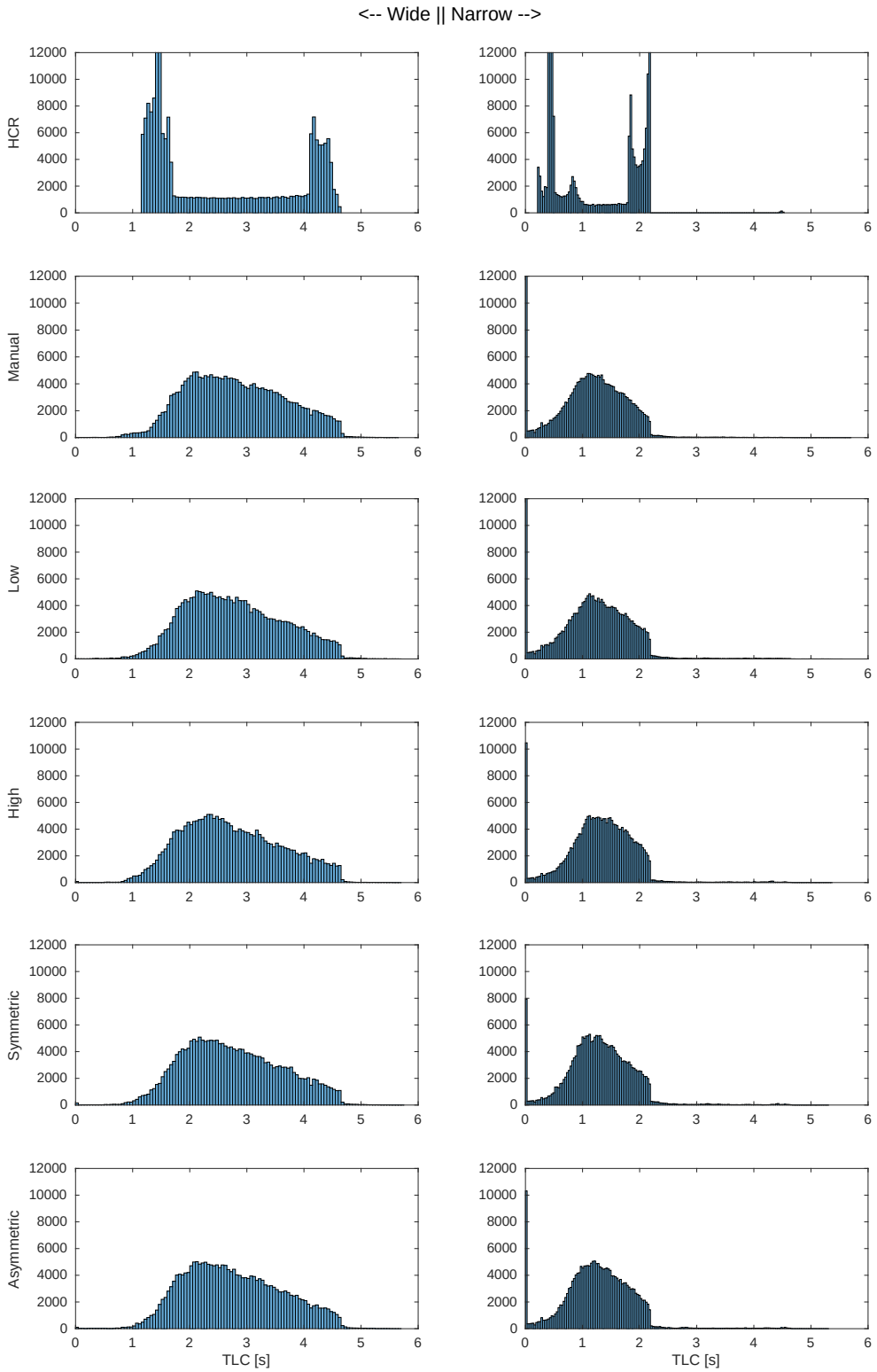

Figure C.5: TLC distribution, take special note of the double peaks of the HCR representing TLC on straights and curves. The relatively small buffer between the curve peak and a TLC of 0 may explain the limited effect of LoHA controllers on the safety margins.

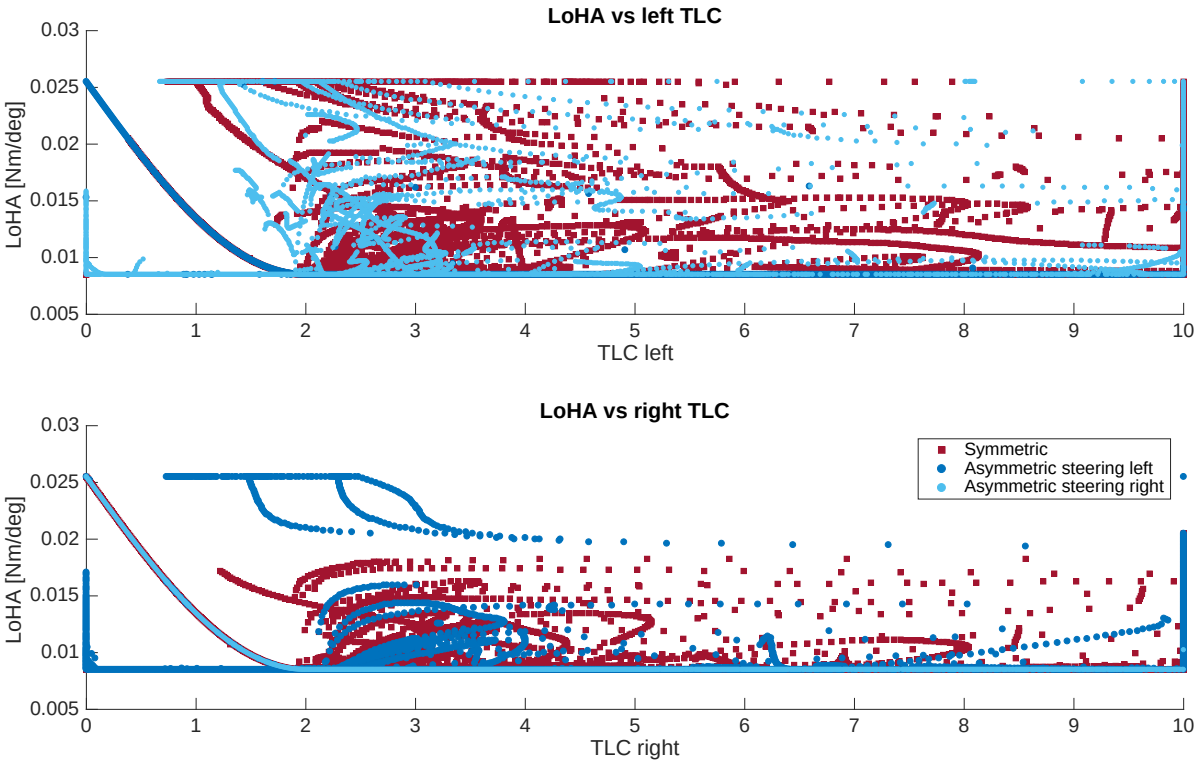

Figure C.6: Controller LoHA

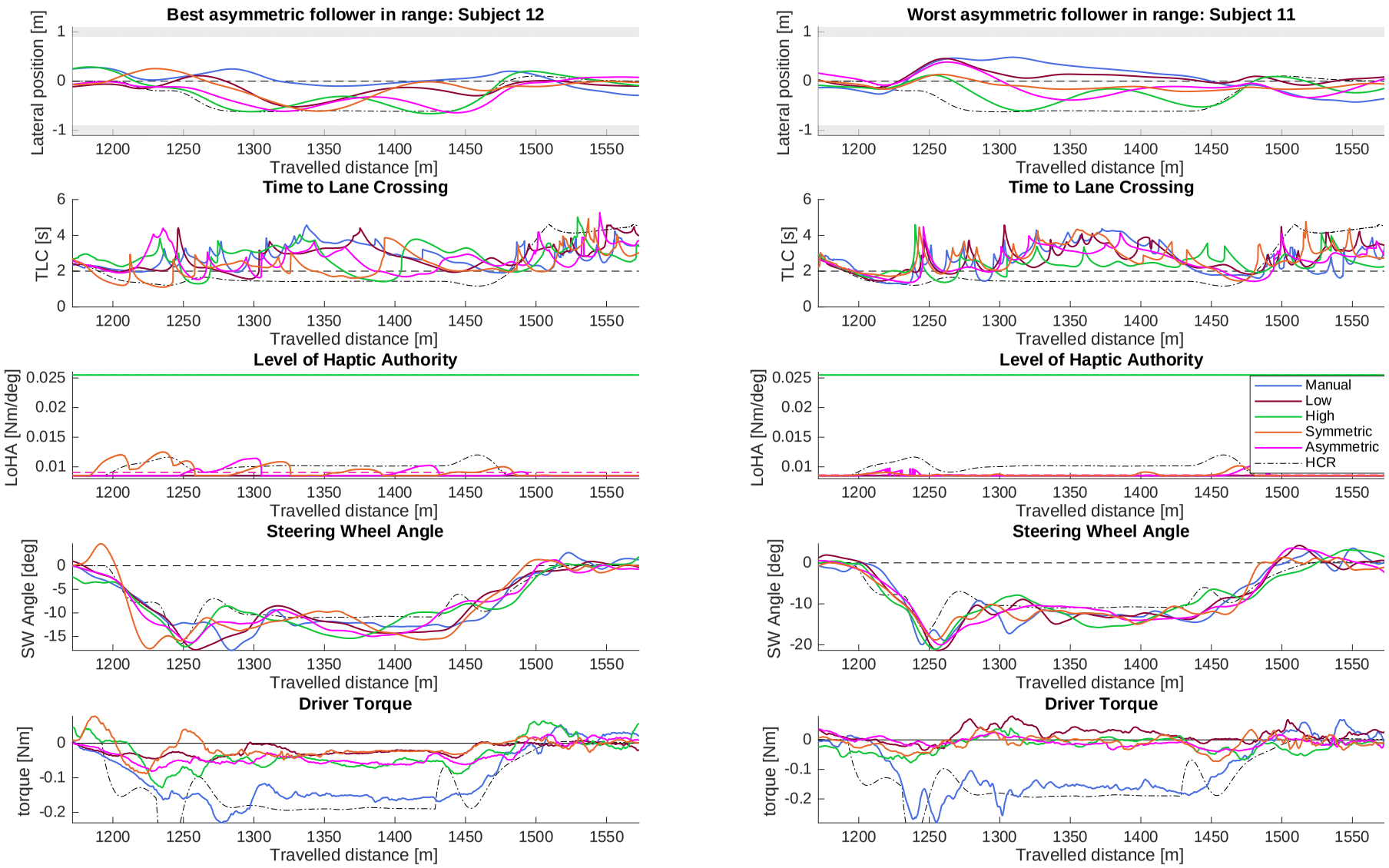

Figure C.7: Data recording for the best and worst asymmetric followers on the wide right curve, pay special attention to the driver torques and the conflicts between following the HCR and staying away.

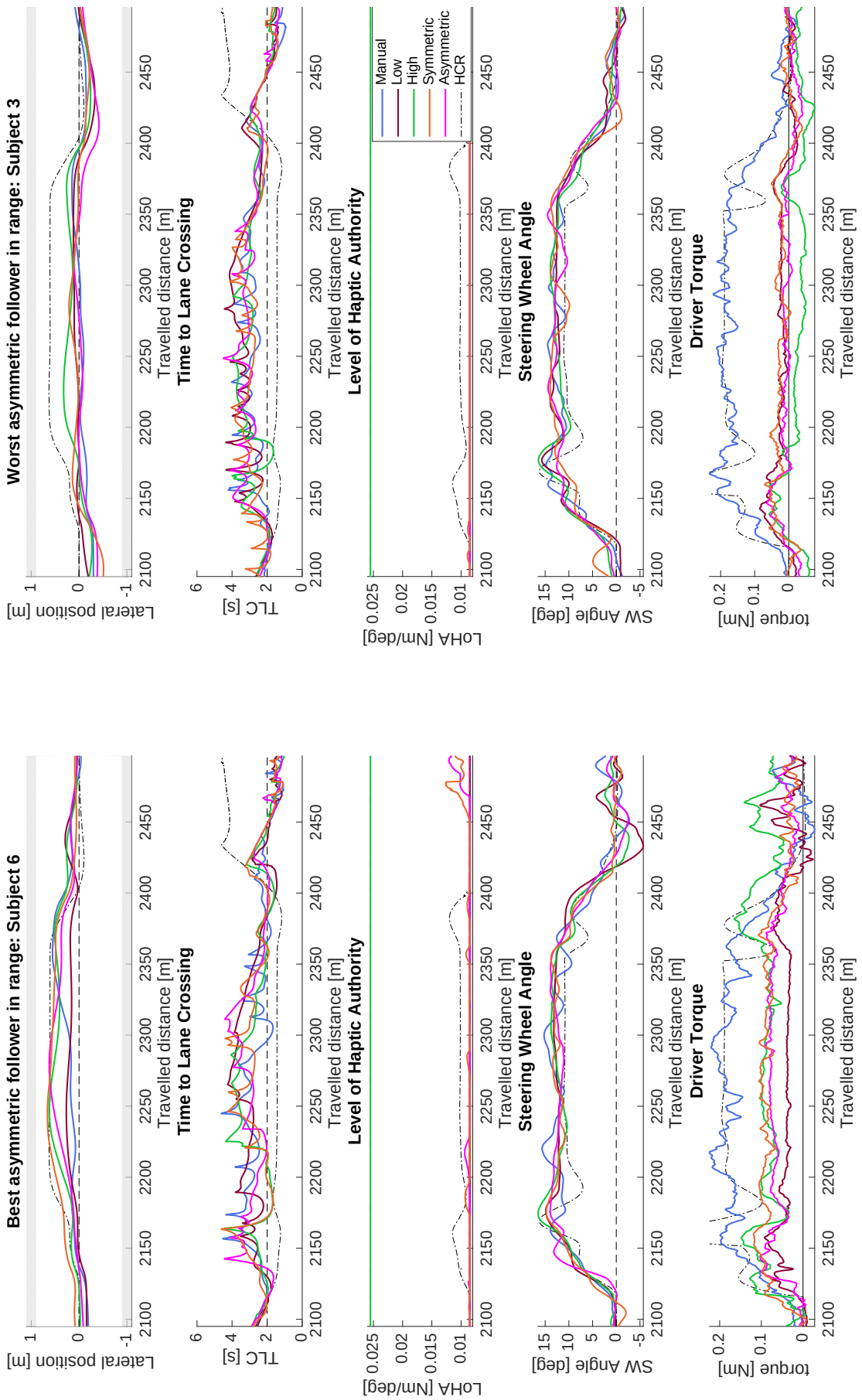

Figure C.8: Data recording for the best and worst asymmetric followers on the wide left curve

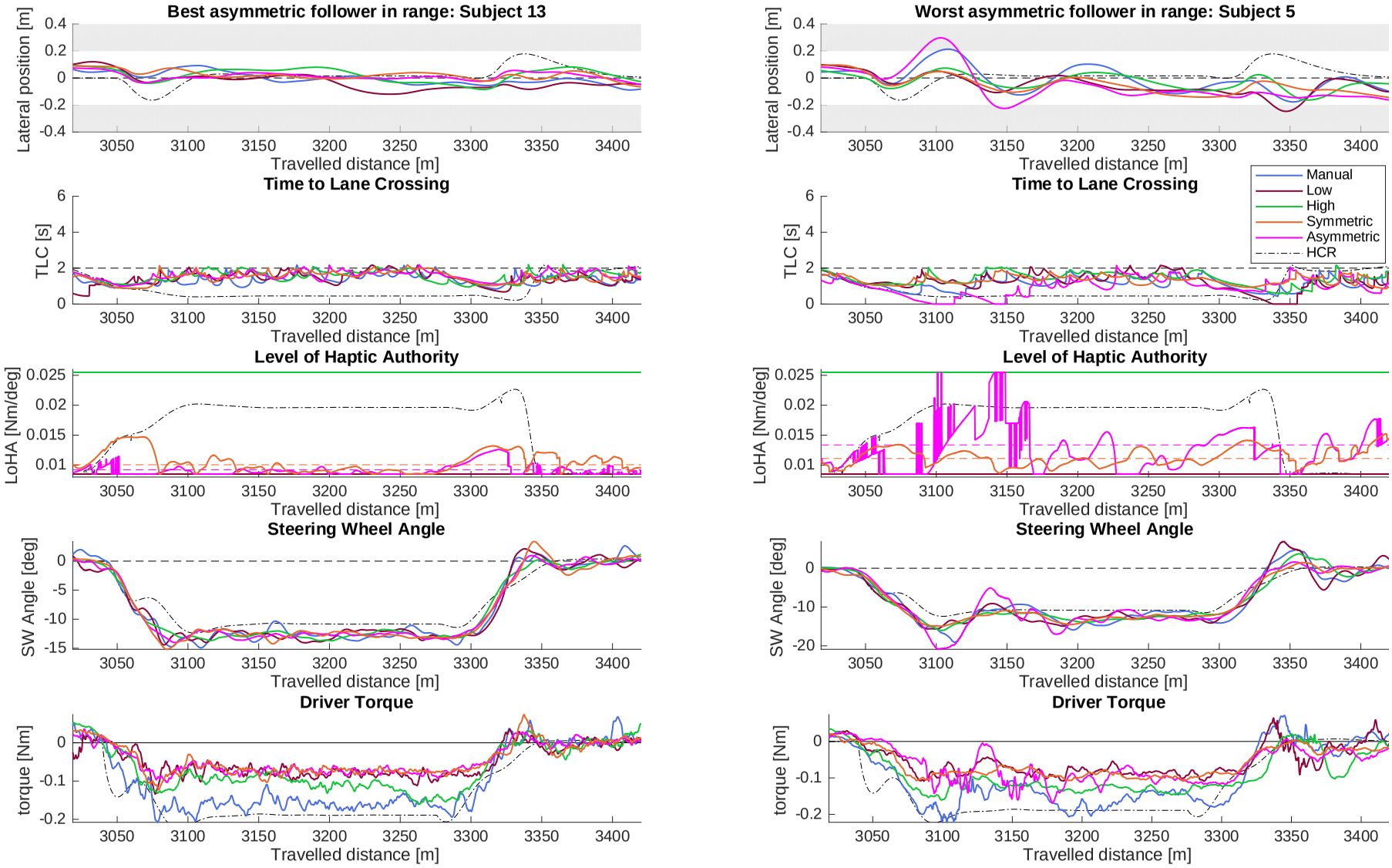

Figure C.9: Data recording for the best and worst asymmetric followers on the narrow right curve

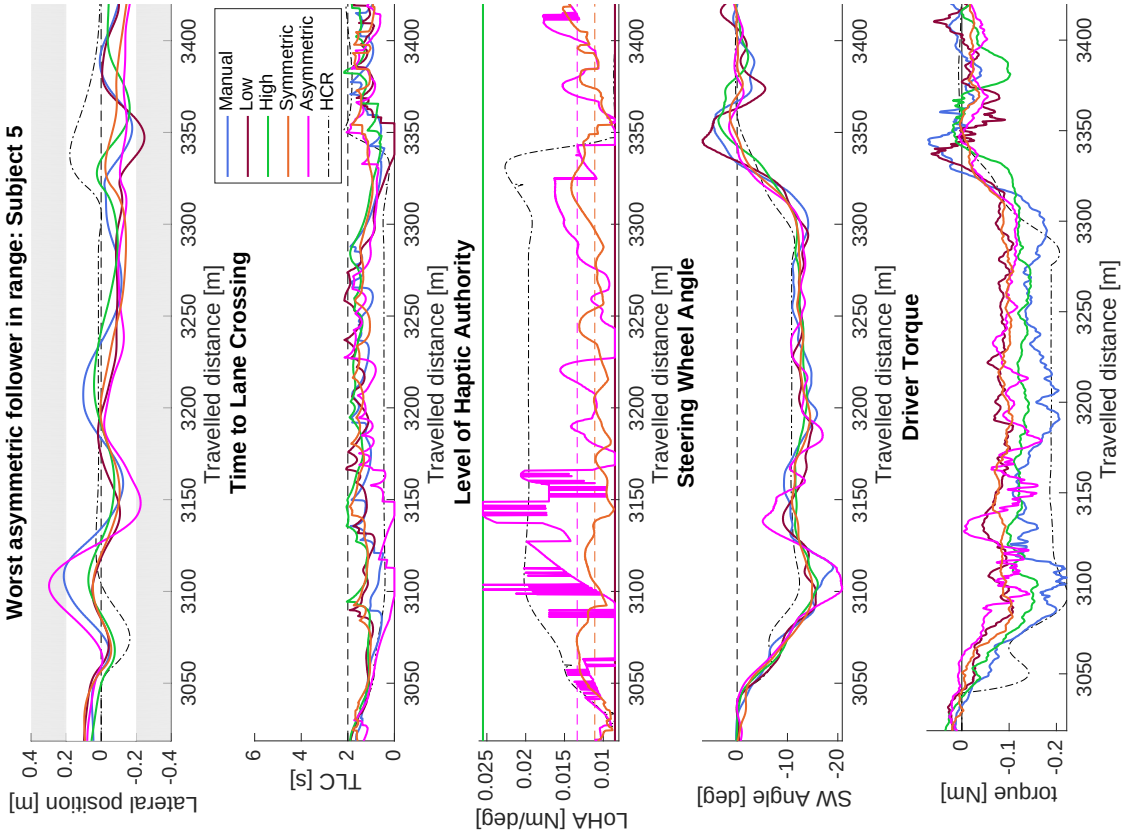

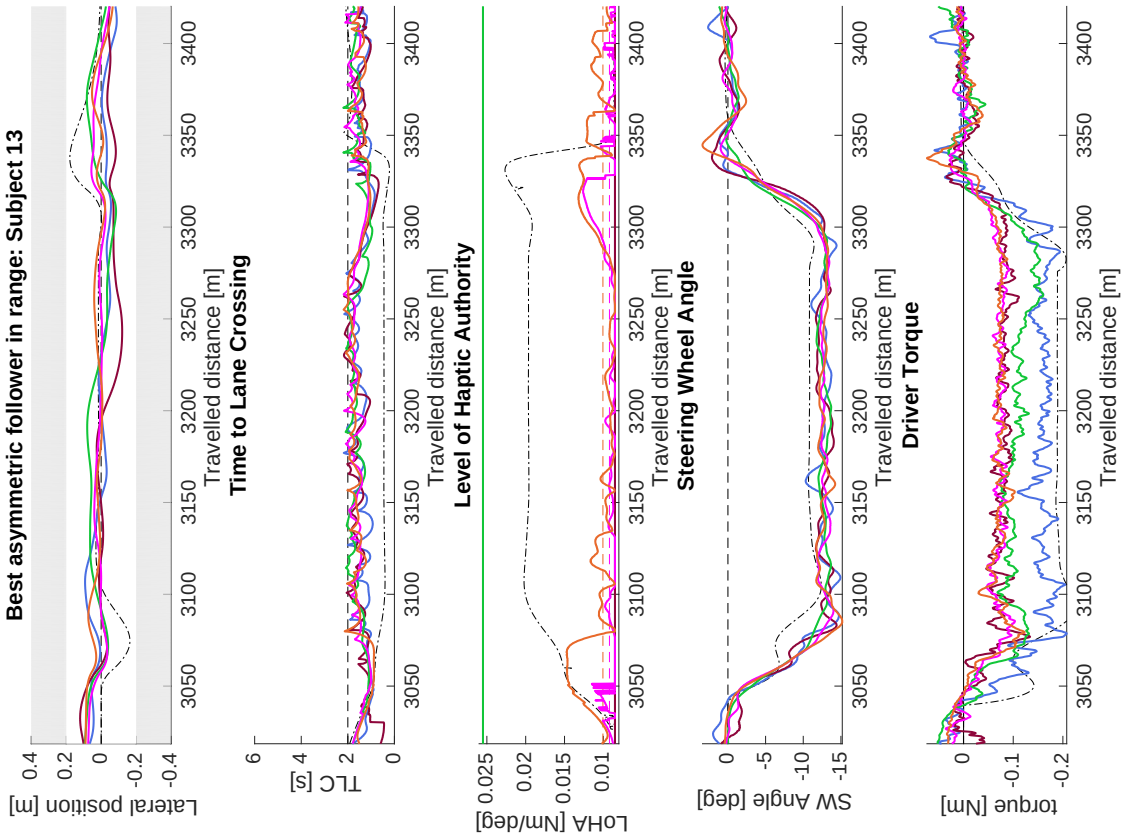

Figure C.10: Data recording for the best and worst asymmetric followers on the narrow left curve

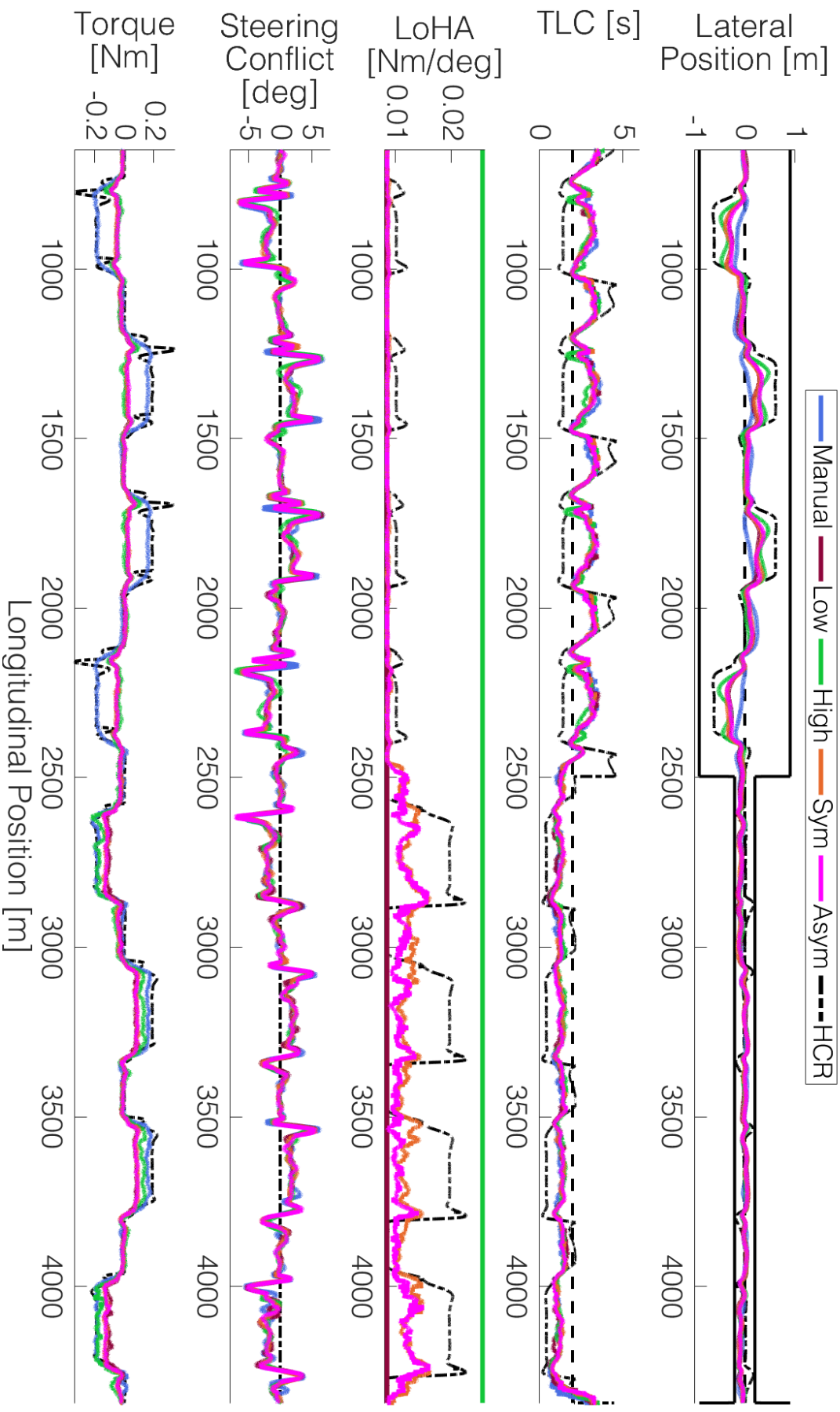

Figure C.11: Time trace average over all subjects separated by controller.

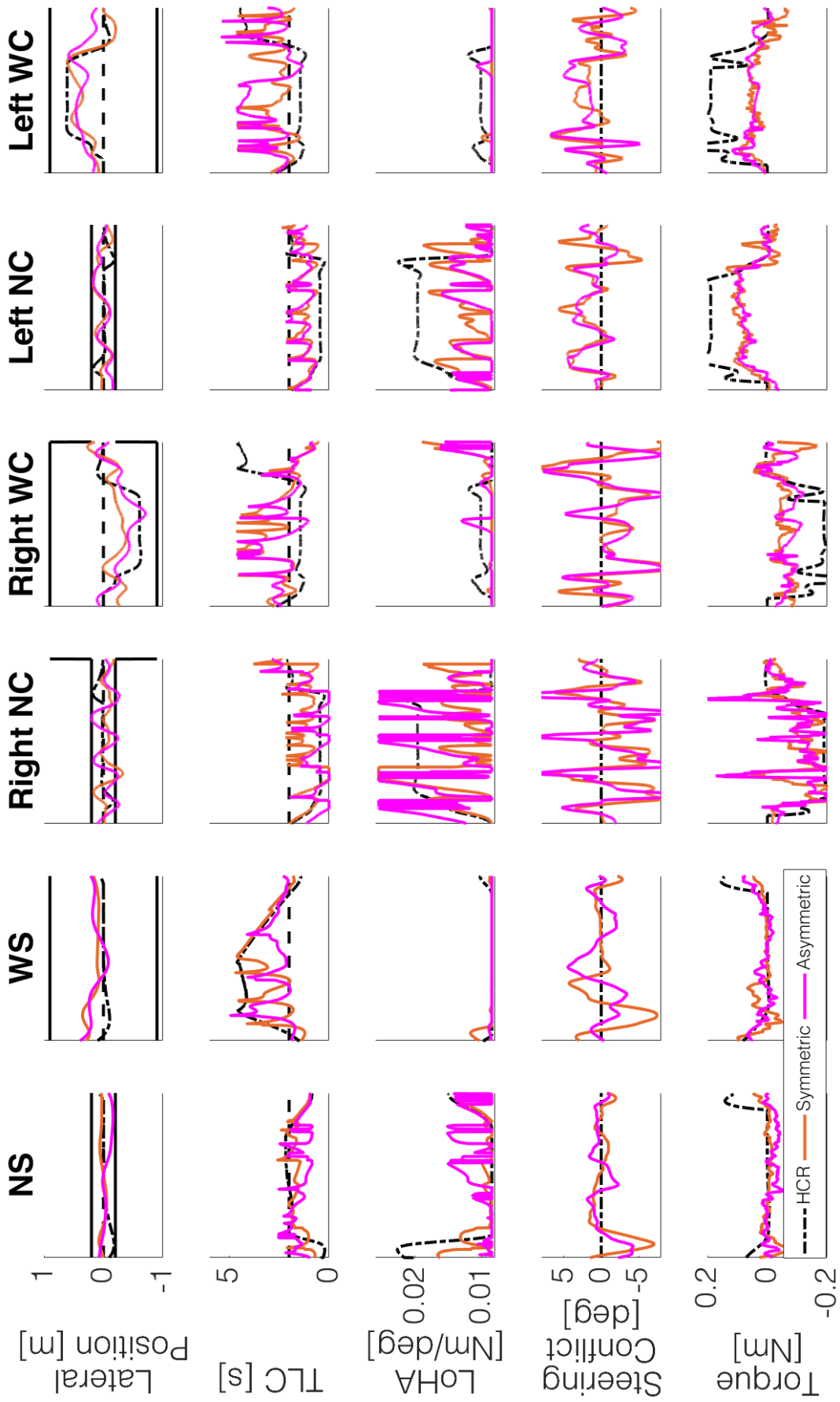

Figure C.12: Seperate time trace of subject 1 with a symmetric and asymmetric adaptive controller over all different road sections.

D

Participant forms

VAN DER LAAN QUESTIONAIRE

I find the system (please tick a box on every line):

1	Useful	|__|__|__|__|__|	Useless
2	Pleasant	|__|__|__|__|__|	Unpleasant
3	Bad	|__|__|__|__|__|	Good
4	Nice	|__|__|__|__|__|	Annoying
5	Effective	|__|__|__|__|__|	Superfluous
6	Irritating	|__|__|__|__|__|	Likeable
7	Assisting	|__|__|__|__|__|	Worthless
8	Undesirable	|__|__|__|__|__|	Desirable
9	Raising Alertness	|__|__|__|__|__|	Sleep inducing

Comments on the experiment and system:

……

……

……

……

……

……

……

To be filled out by the researcher:

Participant nr:	Condition nr:	Date:

Van der Laan, J.D., Heino, A., & De Waard, D. (1997). A simple procedure for the assessment of acceptance of advanced transport telematics. Transportation Research - Part C: Emerging Technologies, 5, 1-10.

Figure 8.6

NASA Task Load Index

Hart and Staveland's NASA Task Load Index (TLX) method assesses work load on five 7-point scales. Increments of high, medium and low estimates for each point result in 21 gradations on the scales.

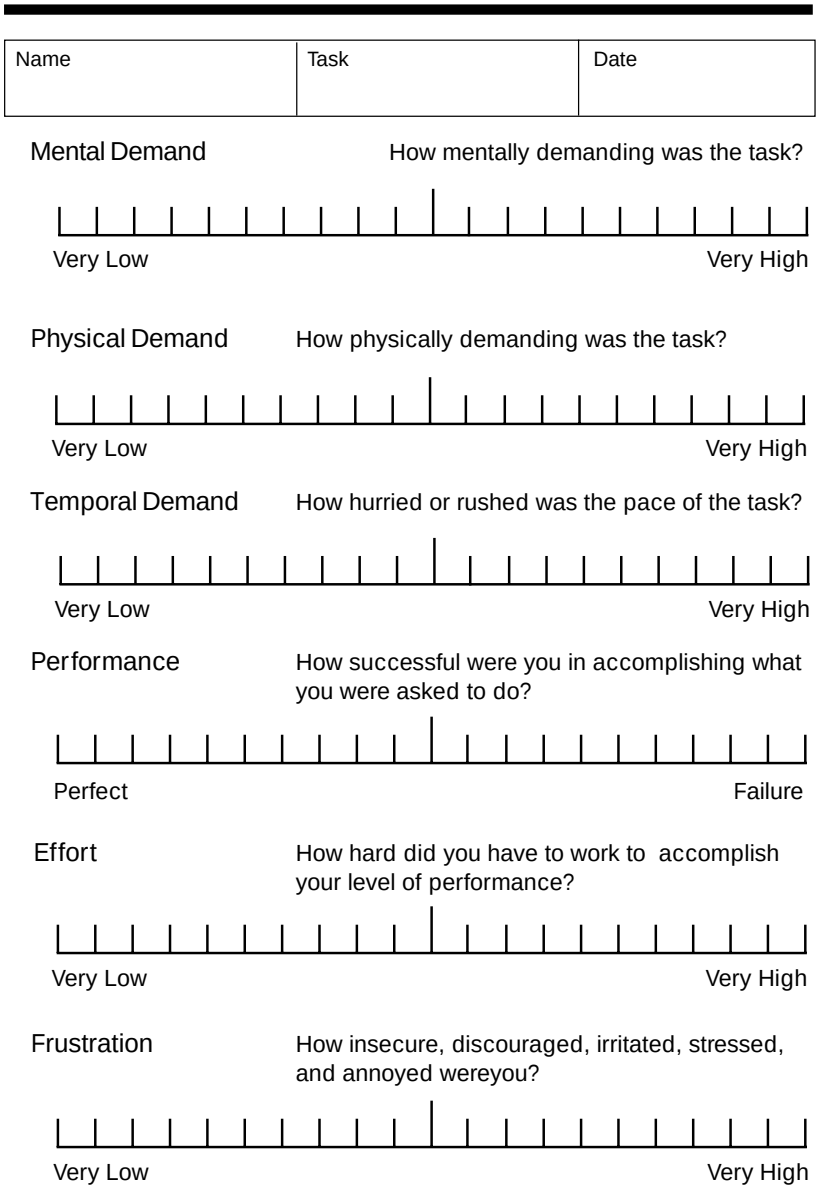

INFORMED CONSENT FORM

Researchers
Hugo Zwaan BSc – Principal Researcher
Email: h.m.zwaan@student.tudelft.nl
Tel: +31-6-29579123

Prof dr. ir. D.A. Abbink – Supervisor
Email: d.a.abbink@tudelft.nl

Location
TU Delft, Faculty of Aerospace Engineering
Department of Control and Operations – Control and Simulation
HMI-Lab, room 0.38
Kluyverweg 1
2628 HS Delft

Before agreeing to participate in this study it is important that the information in this document is carefully read and understood! This document will describe the purpose, procedures, risks and possible discomforts of this experiment.

Purpose of the Research
The purpose of this research is to investigate the effect of different controller stiffnesses in driving with haptic shared control on the performance, behavior and comfort of drivers. The haptic device is an actuated steering wheel that can turn itself. Depending on the testing conditions the steering wheel may become easier or more difficult to turn. The results will be statistically analyzed and published in a master thesis, as well as a possible publication.

Procedure
After reading these instructions you will be asked to drive a fixed base driving simulator around a virtual track. You are only tasked with steering the vehicle as the vehicle velocity is fixed by the simulator, the gas and brake pedals are disabled in the simulator. Please keep your hands on the steering wheel at all times in a ten-to-two position.

Two initial test rounds will be used to get acquainted with operation of the simulator as well as the experience of haptic feedback. Followed by five experimental conditions in a randomized order. After each trial you will be asked to fill out a short questionnaire on your experience.

Task Instructions
Drive the entirety of the track as you would normally would in a real car, stay within the lane and avoid hitting any cones. If you hit the cones or drive off-road, the steering wheel will vibrate to indicate this. The simulation will be stopped after the test track ends.

Duration
The totality of the experiment will take around 60 minutes, this includes driving the two training rounds, five test conditions and filling out the questionnaires.

Risks and discomforts
A small percentage of people (<5% of the population) may experience some form of motion sickness, this may include: nausea, drowsiness, fatigue, headache, blurred vision, eyestrain or trouble focusing. If you feel uncomfortable in any way you are advised to take a couple of minute's rest or stop the experiment. An emergency button can be pressed to stop the simulator immediately, make sure to take notice of its location in the simulator.

Confidentiality and privacy
All data will be anonymized and subjects are referred to by only a subject number, data is kept confidential and will be used for research purposes only.

Rights
At any time you have the right to withdraw from the experiment without mentioning any reason or consequences.

Questions
If you have any questions regarding the experiment or research you can contact H.M. Zwaan, any questions about the nature of the different test-conditions can be asked at the end of the experiment.

I have read and understood the information provided above and give permission to process the data for the purpose of the study as described above. I agree to voluntarily participate in this study and know my rights to withdraw.

Name: **Signature:**

Date: ____ - ____ - 2018 _____

Participant number:

(To be filled by the researcher)

Simulator Study Personal details

Please make sure you fill out the questionaire before the driving experiment

1. **First and last name**

2. **Gender**
   Mark only one oval.
   - Male
   - Female
   - Prefer not to say

3. **Age**

4. **At which age did you first obtain your driving license?**

5. **On average, how often did you drive a car in the last 12 months?**
   Mark only one oval.
   - Daily
   - 4-6 times per week
   - 1-3 times per week
   - Between once a week and once a month
   - Less than once a month
   - Never
   - Prefer not to say

6. **How many kilometers did you drive in the last 12 months?**
   Mark only one oval.
   - 0
   - 1-1.000
   - 1.001-5.000
   - 5.001-10.000
   - 10.001-20.000
   - 20.001-50.000
   - 50.001-100.000
   - over a 100.000
   - Prefer not to say

7. **Some cars are equipped with Adaptive Cruise Control (ACC), how often did you drive with ACC in the last 12 months?**
Mark only one oval.

- Daily
- 4-6 times per week
- 1-3 times per week
- Between once a week and once a month
- Less than once a month
- Never
- I don't know what Adaptive Cruise Control is
- Prefer not to say

8. **Some cars are equipped with Lane Keeping Assistance (LKA), how often did you drive with LKA in the last 12 months?**
Mark only one oval.

- Daily
- 4-6 times per week
- 1-3 times per week
- Between once a week and once a month
- Less than once a month
- Never
- I don't know what Lane Keeping Assistance is
- Prefer not to say

9. **How many accidents were you involved in when driving a car in the last three years?**
Mark only one oval.

- 0
- 1
- 2
- 3
- 4
- 5 or more
- Prefer not to say

10. **Have many times have you driven in a driving simulator?**
Mark only one oval.

- 0
- 1
- 2
- 3
- 4
- 5 or more

11. **How many times have you driven THIS driving simulator?**

Mark only one oval.

- 0
- 1
- 2
- 3
- 4
- 5 or more

Powered by
Google Forms